Supporting Information

Self-Assembly of a Tetraphenylethylene-Based Capsule Showing Both Aggregation- and Encapsulation-Induced Emission Properties

Ting Zhang, Guang-Lu Zhang, Qian-Qian Yan, Li-Peng Zhou, Li-Xuan Cai, Xiao-Qing Guo, Qing-Fu Sun *

Corresponding Email: qfsun@fjirsm.ac.cn

Contents

1. General

Unless otherwise noted, all chemicals and solvents were purchased from commercial corporations and used without further purification. Deuterated solvents were purchased from Admas and J&K scientific. 1D and 2D NMR spectra were measured on a Bruker Biospin Avance III (400 MHz) spectrometer. 1H NMR chemical shifts were determined with respect to residual solvent signals of the deuterated solvents used. ESI-TOF mass spectra were recorded on an Impact II UHR-TOF mass spectrometry from Bruker, with ESI-L low concentration tuning mix (from Agilent Technologies) as the internal standard (Accuracy < 3 ppm). Data analyses and simulations of ESI-TOF mass spectra were processed on a Bruker Data Analysis software (Version 4.3). UV-visible absorption spectra were measured on a UV-2700 spectrophotometer from SHIMADZU. Fluorescent spectra were measured on a FS5 spectrofluorometer from Edinburgh Instruments Ltd. The emission quantum yields in solution and solid state were measured by FS5 Spectro Fluorometer from Edinburg Photonics with integrating sphere. The purity of the ligand L was determined using an SHIMADZU LC20A HPLC instrument with a InertSustain C18 (5μm, 4.6 mm * 250 mm; Daicel Corporation, China), using mobile phase of methanol at a flow rate of 0.5 mL/min. The retention time of the ligand L was 8.24 min. The purity determined by integrating HPLC–UV absorption peaks (300 nm) was 100% for the L. Dynamic light scattering (DLS) spectra were recorded on a Malvern Nanosizer S instrument at room temperature.

Synthesis of $Pd_2L_4(BF_4)_4$

Ligand **L** (9.76mg, 20.08μmol) was treated with $Pd(CH_3CN)_4(BF_4)_2$ (10.04 μmol) in DMSO (1mL) at 70 °C for 3 h and a light yellow solution was obtained. ^{1}H NMR confirmed the quantitative formation of the complex. ^{1}H NMR (400 MHz, [D_6]DMSO, 298K) δ 9.38 (s, 8H), 9.25 (d, J = 5.4 Hz, 8H), 8.22 (d, J = 8.0 Hz, 8H), 7.81 – 7.74 (m, 8H), 7.37 (d, J = 8.1 Hz, 16H), 7.23 – 7.07 (m, 40H), 6.95 (d, J = 7.3 Hz, 16H).

Synthesis of $Pd_2L_4(PF_6)_4$

Ligand **L** (9.76mg, 20.08μmol) was treated with $Pd(PF_6)_2$ (10.04 μmol) in DMSO (1mL) at 70 °C for 3 h and a light yellow solution was obtained. ^{1}H NMR confirmed the quantitative formation of the complex. ^{1}H NMR (400 MHz, [D_6]DMSO, 298K) δ 9.36 (s, 8H), 9.27 (d, J = 5.4 Hz, 8H), 8.21 (d, J = 6.4 Hz, 8H), 7.76 (m, J = 5.5 Hz, 8H), 7.37 (d, J = 5.3 Hz, 16H), 7.25 – 7.06 (m, 40H), 6.95 (d, J = 3.3 Hz, 16H).

Synthesis of $Pd_2L_4(CF_3SO_3)_4$

Ligand **L** (9.76mg, 20.08μmol) was treated with $Pd(CF_3SO_3)_2$ (10.04 μmol) in DMSO (1mL) at 70 °C for 3 h and a light yellow solution was obtained. ^{1}H NMR confirmed the quantitative

formation of the complex. ^{1}H NMR (400 MHz, [D_6]DMSO, 298K) δ 9.35 (s, 8H), 9.26 (d, J = 2.5 Hz, 8H), 8.23 (d, J = 4.7 Hz, 8H), 7.83 – 7.74 (m, 8H), 7.37 (d, J = 5.8 Hz, 16H), 7.15 (dd, J = 29.1, 11.2 Hz, 40H), 6.96 (d, J = 6.3 Hz, 16H).

2. Single crystal X-ray diffraction study

Crystals suitable for analysis by X-ray diffraction grew at room temperature over two weeks by gas phase diffusion of ethyl acetate into a DMSO solution of the complex **1**$(NO_3)_4$. The crystal was found to decompose quickly in air. A yellow crystal was taken out from the mother liquor and transferred instantly into a glass-capillary and flame-sealed. Cell determination and data collection were performed on a supernova diffractometer equipped with a Multilayers mirror Cu-Kα radiation (λ = 1.5418 Å). The crystal structure was solved by direct method and refined by full-matrix least squares on F^2 using *SHELX* package.[S1] Solvent molecules are highly disordered and attempts to locate and refine the solvent peaks were unsuccessful. The diffused electron densities resulting from these solvent molecules were removed using the *SQUEEZE* routine of *PLATON*.[S2]

Crystal data and structure refinement results for $Pd_2L_4(NO_3)_4$ were summarized in Table S1. The X-ray crystallographic coordinates for structures reported in this Article have been deposited at the Cambridge Crystallographic Data Centre (CCDC), under deposition no CCDC 1557886. These data can be obtained free of charge (http://www.ccdc.cam.ac.uk/data_request/cif).

3. Figures and Tables

3.1 Spectra of capsules

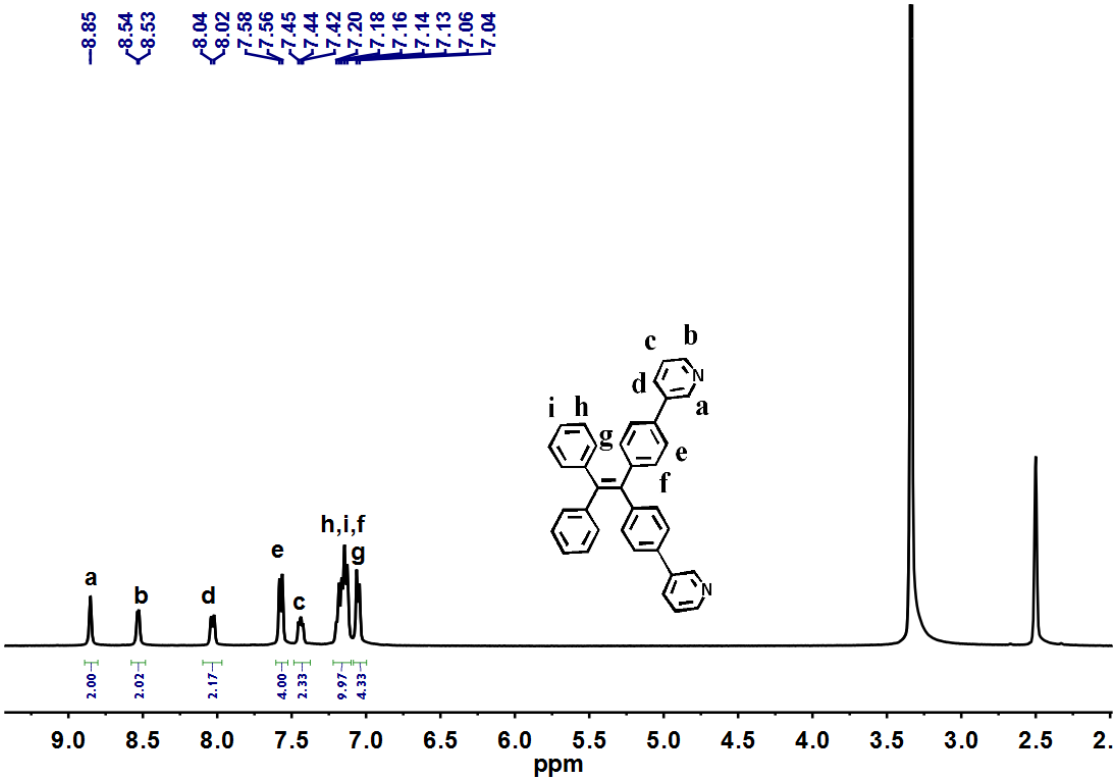

Fig. S1 ^{1}H NMR spectrum of the ligand **L** (400 MHz, [D_6]DMSO, 298K)

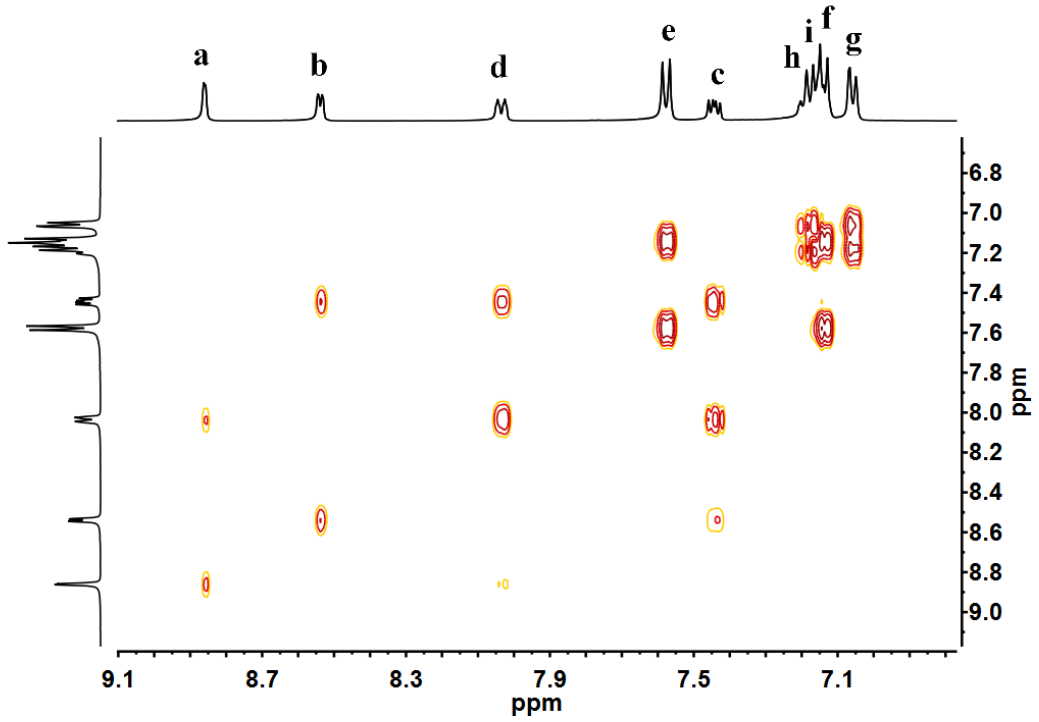

Fig. S2 ^{1}H-^{1}H COSY spectrum of the ligand **L** (400 MHz, [D6]DMSO, 298K).

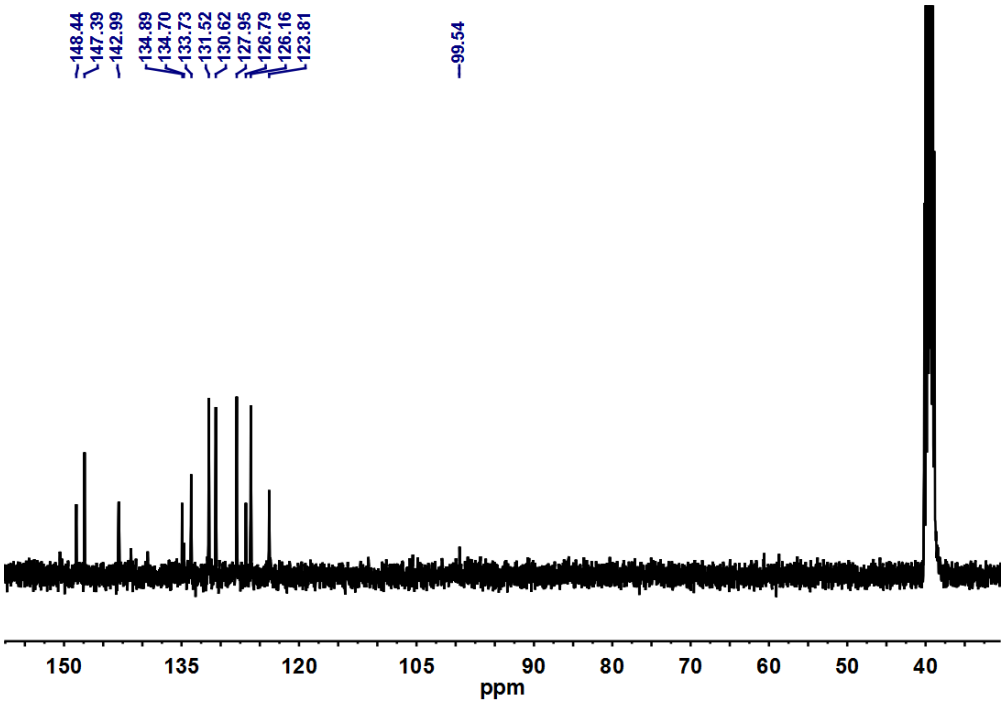

Fig. S3 ^{13}C NMR spectrum of the ligand **L** (100 MHz, [D_6]DMSO, 298K).

SHIMADZU LabSolutions **Analysis Report**

<Sample Information>

Sample Name	: zt411b-3		
Sample ID	:		
Data Filename	: zt411b-3.lcd		
Method Filename	: zt411b-3.lcm		
Batch Filename	:		
Vial #	: 1-1	Sample Type	: Unknown
Injection Volume	: 10 uL		
Date Acquired	: 10/30/2017 5:50:41 PM	Acquired by	: System Administrator
Date Processed	: 10/30/2017 6:50:43 PM	Processed by	: System Administrator

<Chromatogram>

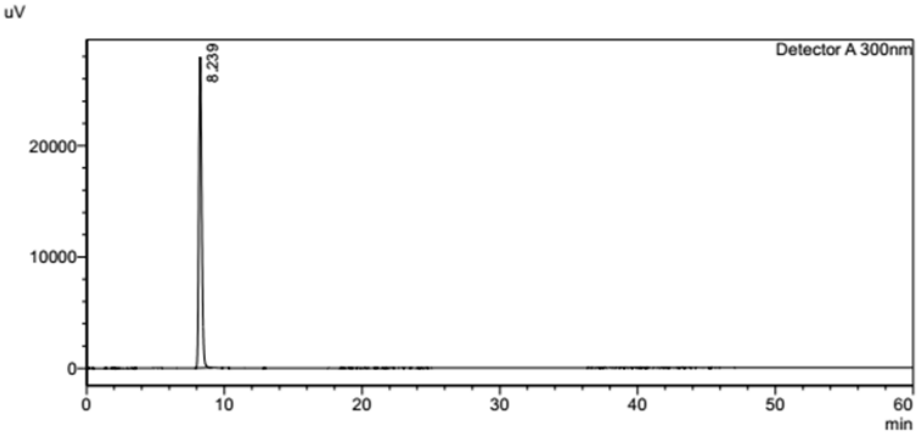

<Peak Table>

Detector A 300nm

Peak#	Ret. Time	Area	Height	Conc.	Unit	Mark	Name
1	8.239	398302	27941	0.000			
Total		398302	27941				

Fig. S4 ^{13}C NMR spectrum of the ligand **L** (100 MHz, [D_6]DMSO, 298K).

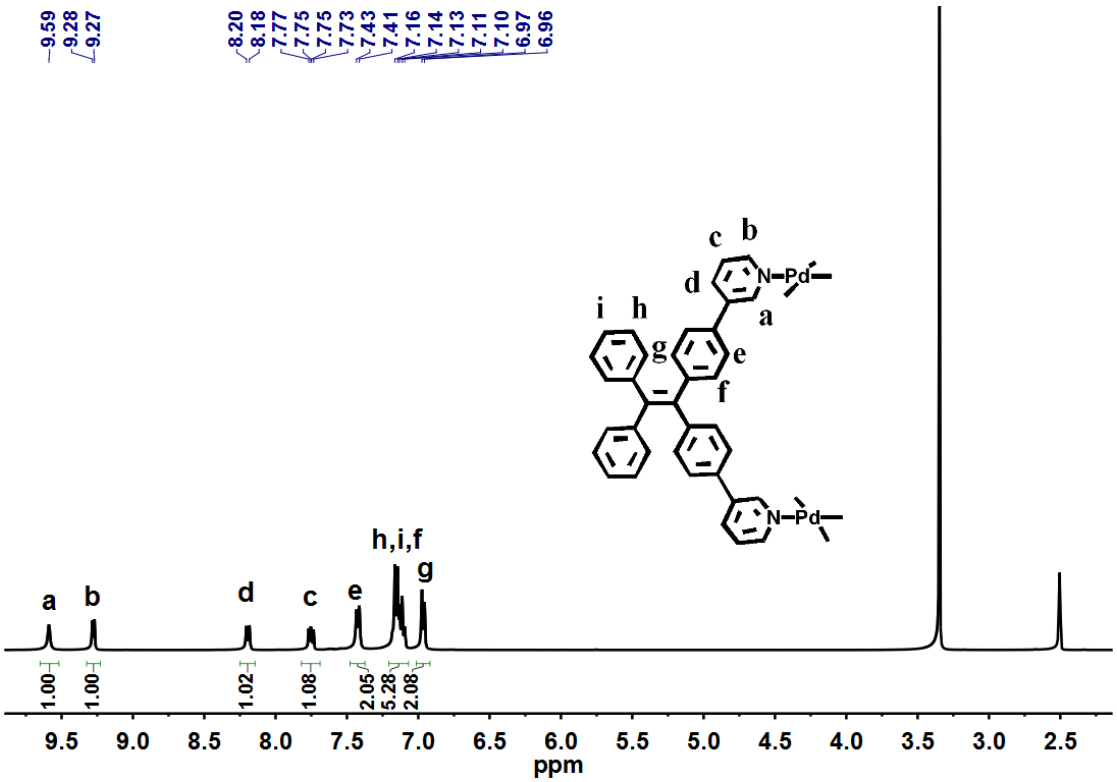

Fig. S5 ^{1}H NMR spectrum of compound $Pd_2L_4(NO_3)_4$(400 MHz, [D_6]DMSO, 298K)

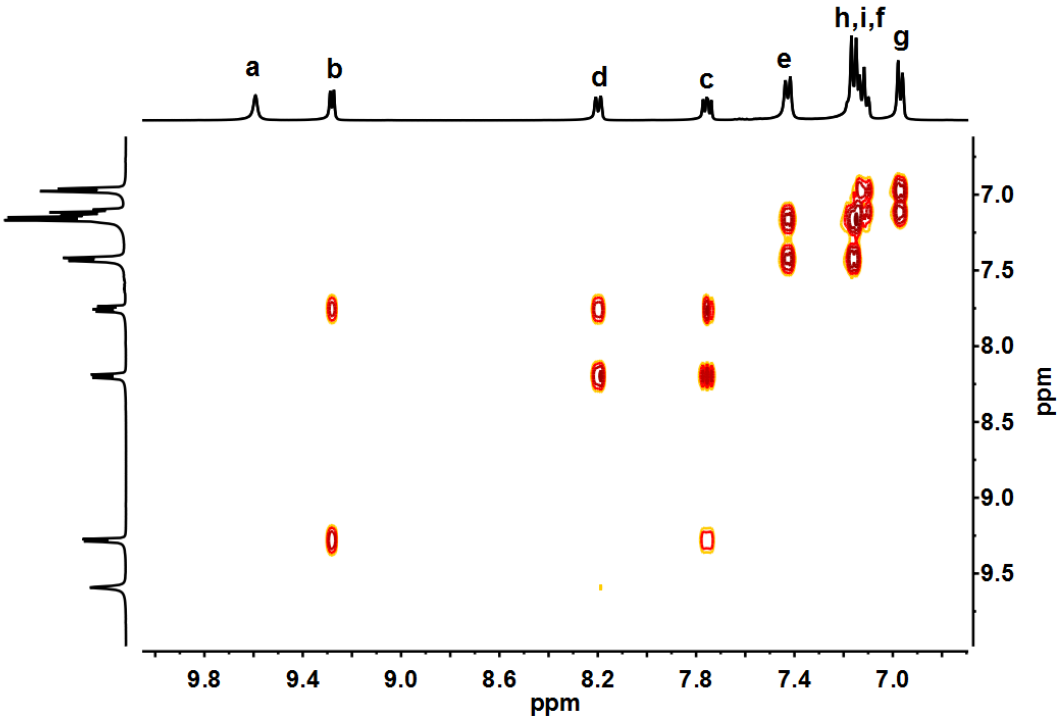

Fig. S6 ^{1}H-^{1}H COSY spectrum of compound $Pd_2L_4(NO_3)_4$ (400 MHz, [D_6]DMSO, 298K)

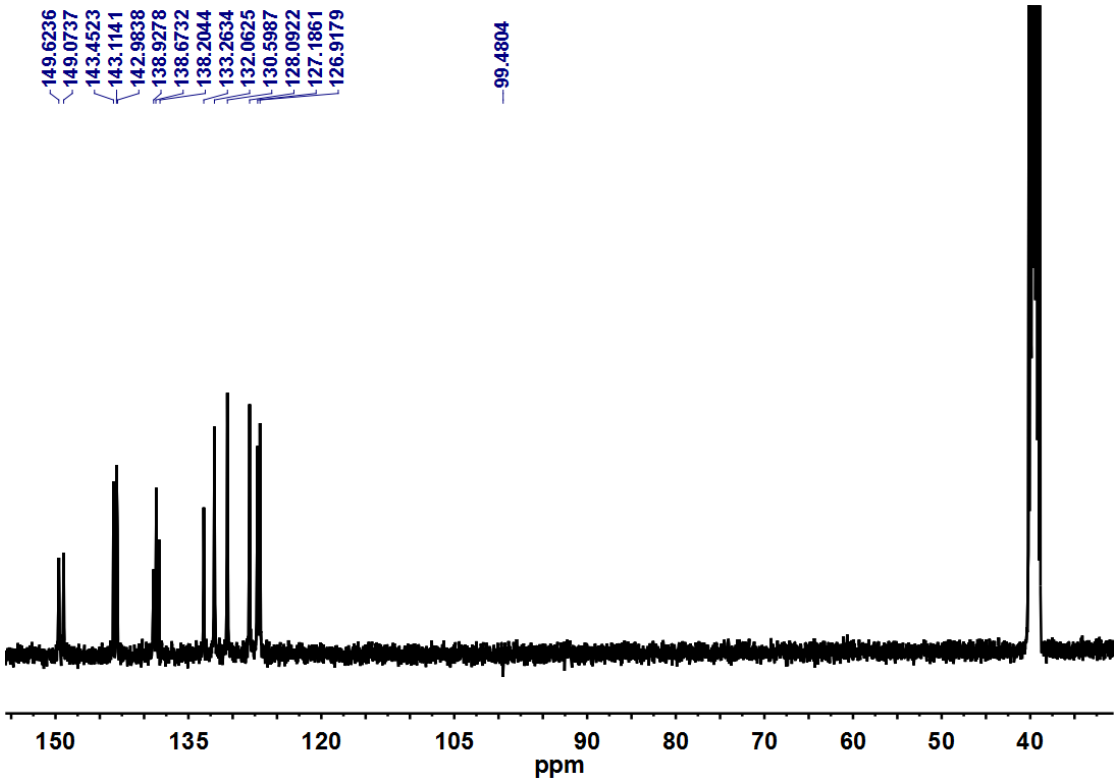

Fig. S7 ^{13}C NMR spectrum of compound $Pd_2L_4(NO_3)_4$ (100 MHz, [D_6]DMSO, 298K)

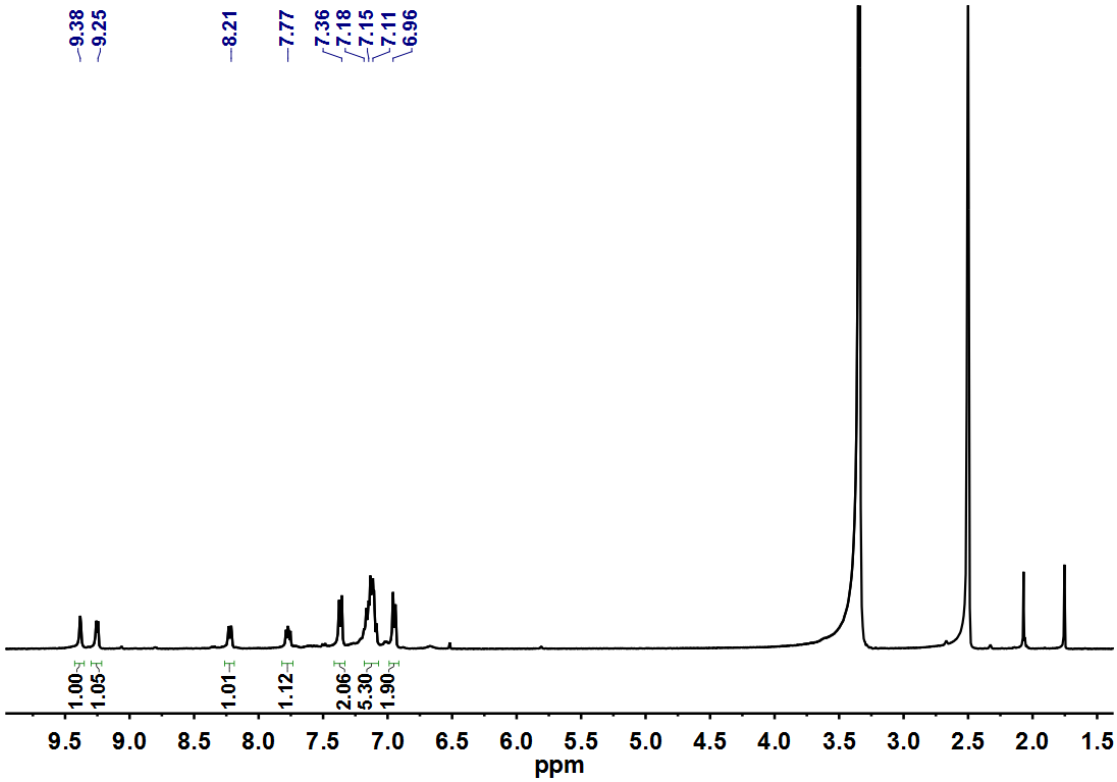

Fig. S8 ^{1}H NMR spectrum of compound $Pd_2L_4(BF_4)_4$ (400 MHz, [D_6]DMSO, 298K)

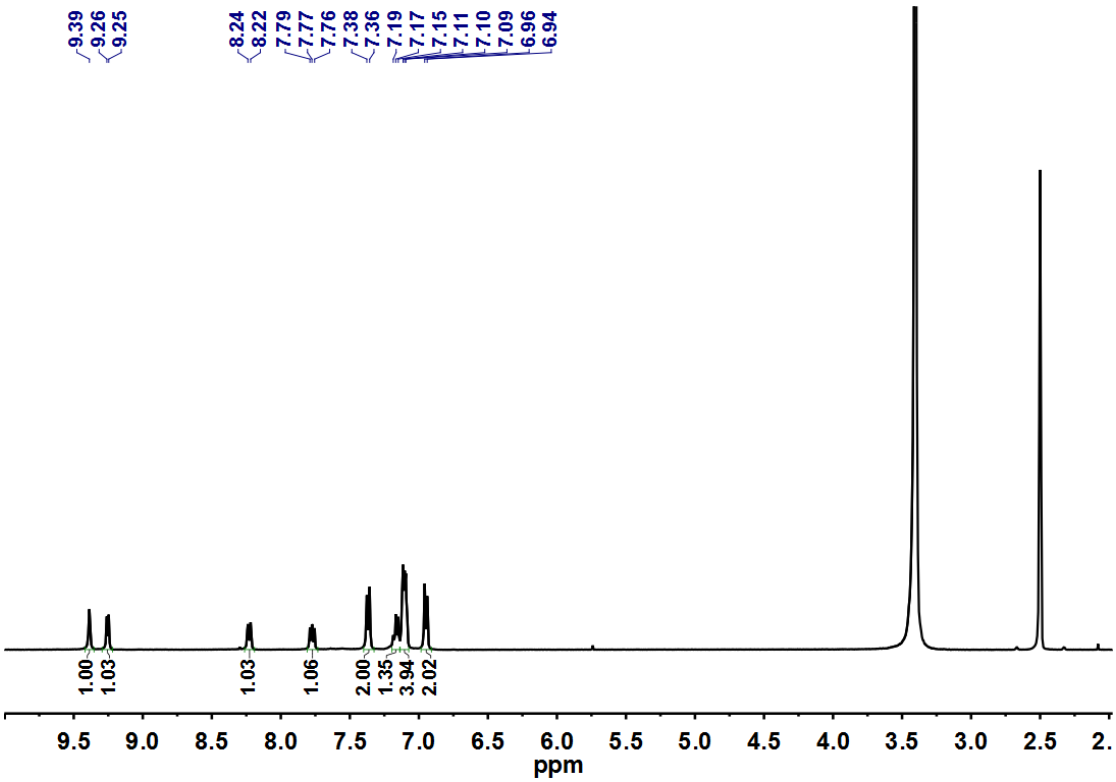

Fig. S9 ^{1}H NMR spectrum of compound $Pd_2L_4(CF_3SO_3)_4$ (400 MHz, [D_6]DMSO, 298K)

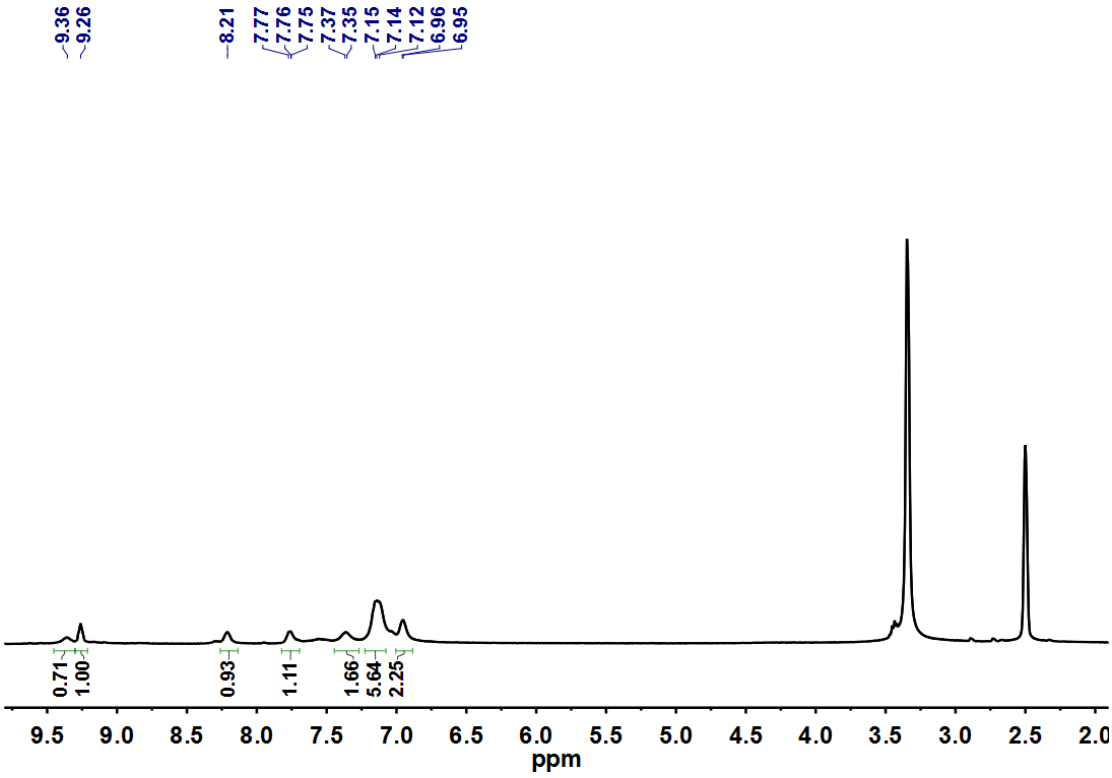

Fig. S10 ^{1}H NMR spectrum of compound $Pd_2L_4(PF_6)_4$(400 MHz, [D_6]DMSO, 298K)

DOSY spectra

Stokes-Einstein equation:

$$D = \frac{k_B T}{6\pi\eta r}$$

was applied to estimate the dynamic radius for the compound $\mathbf{Pd_2L_4}(NO_3)_4$. D is diffusion coefficient obtained from DOSY spectrum, k_B is Boltzmann constant, T is temperature, viscosity tested to be 1.996 mPa•s, and r is the estimated dynamic radius.

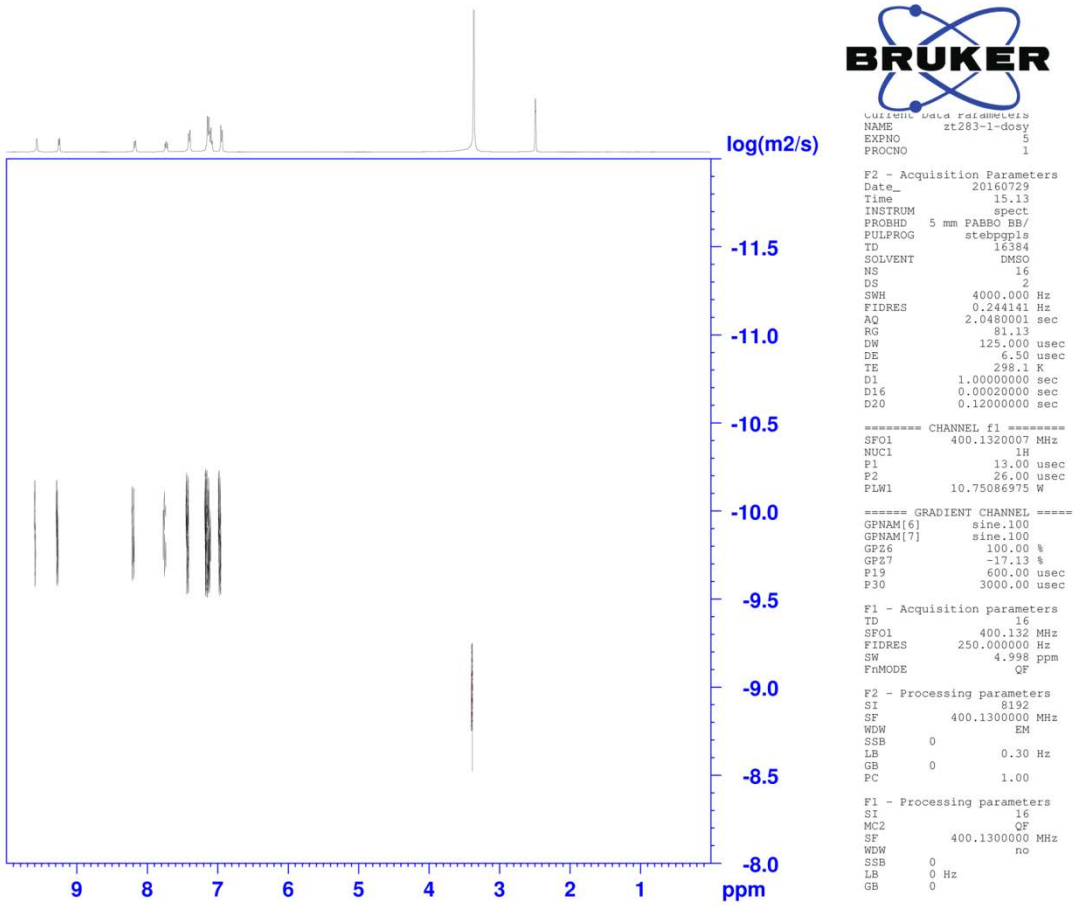

Fig. S11 ^{1}H DOSY spectrum of compound $Pd_2L_4(NO_3)_4$ (400 MHz, [D_6]DMSO, 298K)

Diffusion Constant = 1.486E-10 m^2/S d=1.47 nm

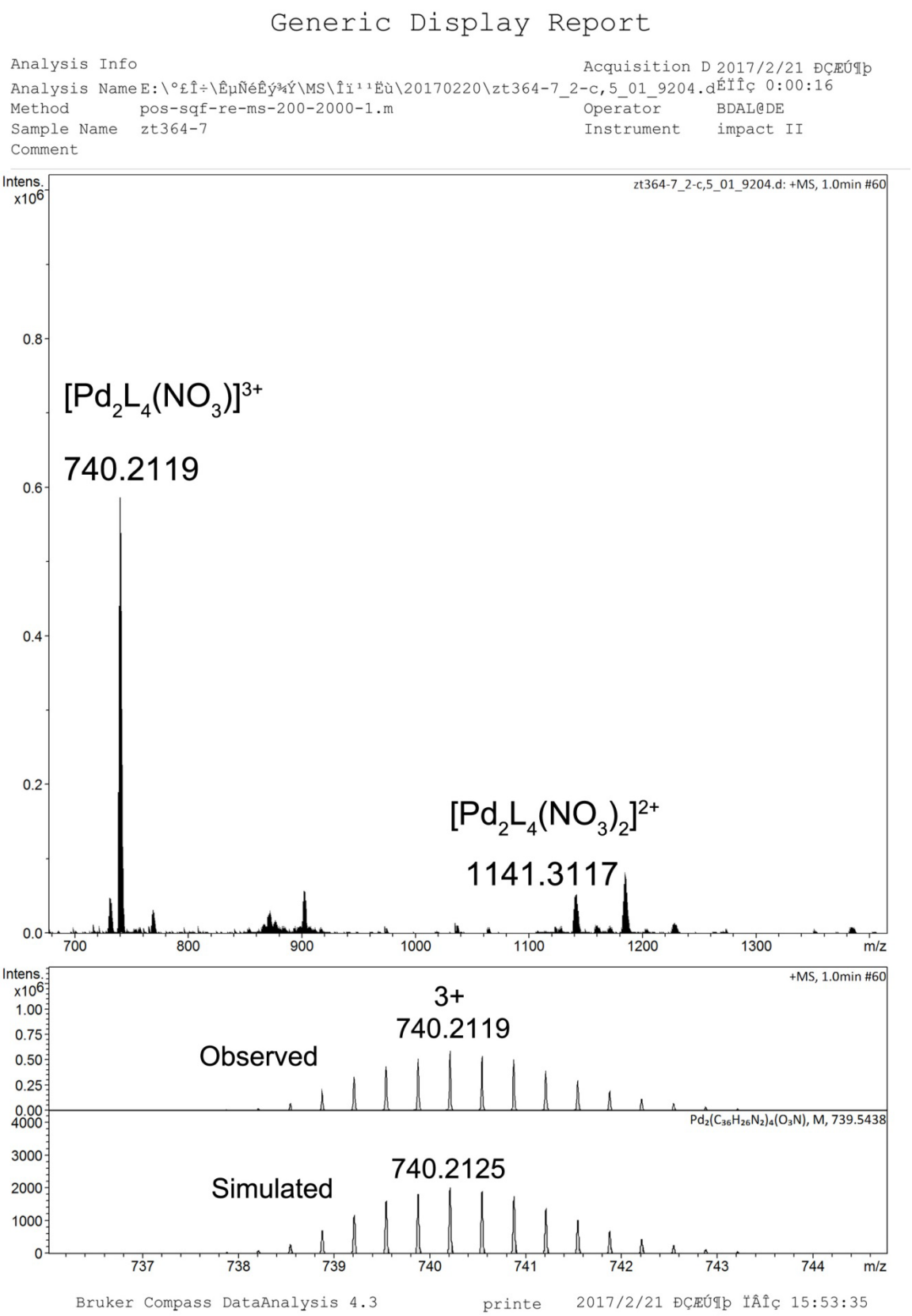

Fig. S12 ESI-TOF mass spectrum of $Pd_2L_4(NO_3)_4$ and the observed and simulated isotope patterns of the 3+ peaks.

X-ray table and figure

Table S1 Crystal data and structure refinement for $Pd_2L_4(NO_3^-$ salt).

CCDC no.	1557886	
Empirical formula	C144 H104 N12 O12 Pd2	
Formula weight	2407.19	
Temperature	293(2) K	
Wavelength	1.54184 Å	
Crystal system	Monoclinic	
Space group	$P2_1/c$	
Unit cell dimensions	a = 21.9948(3) Å	α= 90°.
	b = 10.94353(18) Å	β= 100.8053(13)°.
	c = 37.9712(5) Å	γ = 90°.
Volume	8977.7(2) $Å^3$	
Z	2	
Density (calculated)	0.890 Mg/m^3	
Absorption coefficient	1.951 mm^{-1}	
F(000)	2480	
Crystal size	0.08 x 0.02 x 0.02 mm^3	
Theta range for data collection	3.409 to 74.514°.	
Index ranges	-27<=h<=26, -13<=k<=8, -46<=l<=37	
Reflections collected	33538	
Independent reflections	17704 [R(int) = 0.0358]	
Completeness to theta = 67.684°	99.3 %	
Refinement method	Full-matrix least-squares on F^2	
Data / restraints / parameters	17704 / 126 / 803	
Goodness-of-fit on F^2	1.027	
Final R indices [I>2sigma(I)]	R1 = 0.0549, wR2 = 0.1625	
R indices (all data)	R1 = 0.0723, wR2 = 0.1768	
Extinction coefficient	n/a	
Largest diff. peak and hole	0.815 and -0.795 e.$Å^{-3}$	

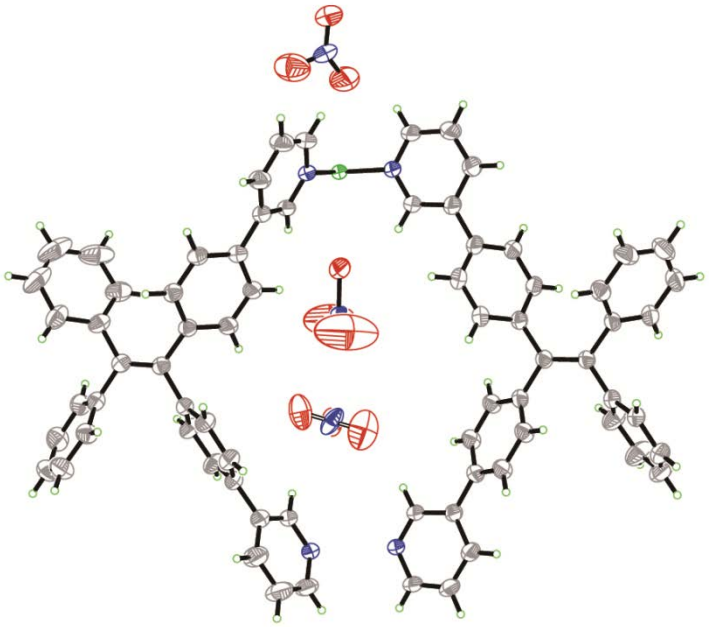

Fig. S13 Ortep-drawing of the asymmetric unit of complex 1 at 30% probability level.

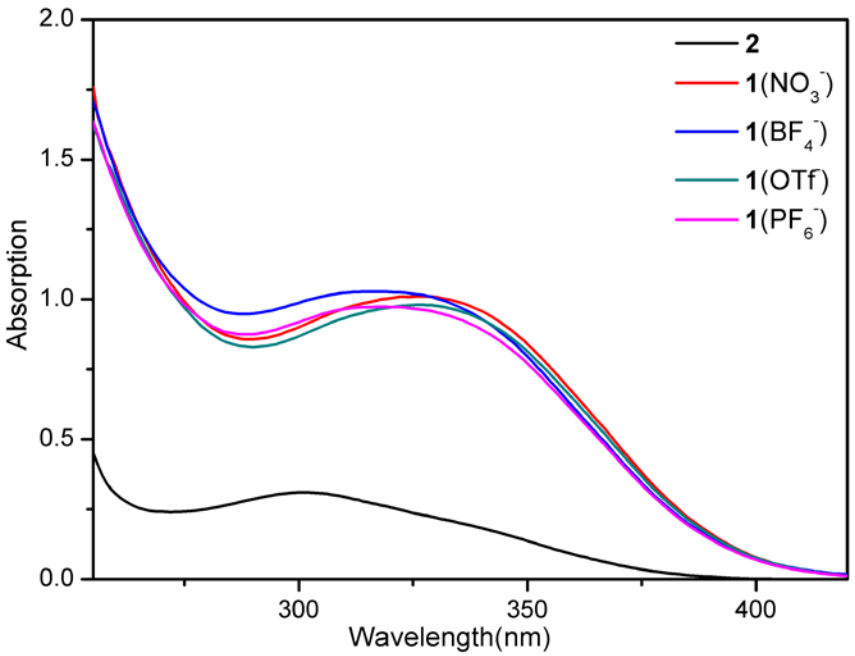

Fig. S14 UV-vis absorption spectra of ligand **L** and complex $Pd_2L_4(NO_3)_4$, $Pd_2L_4(BF_4)_4$, $Pd_2L_4(PF_6)_4$ and $Pd_2L_4(CF_3SO_3)_4$ (c = 10^{-5} M).

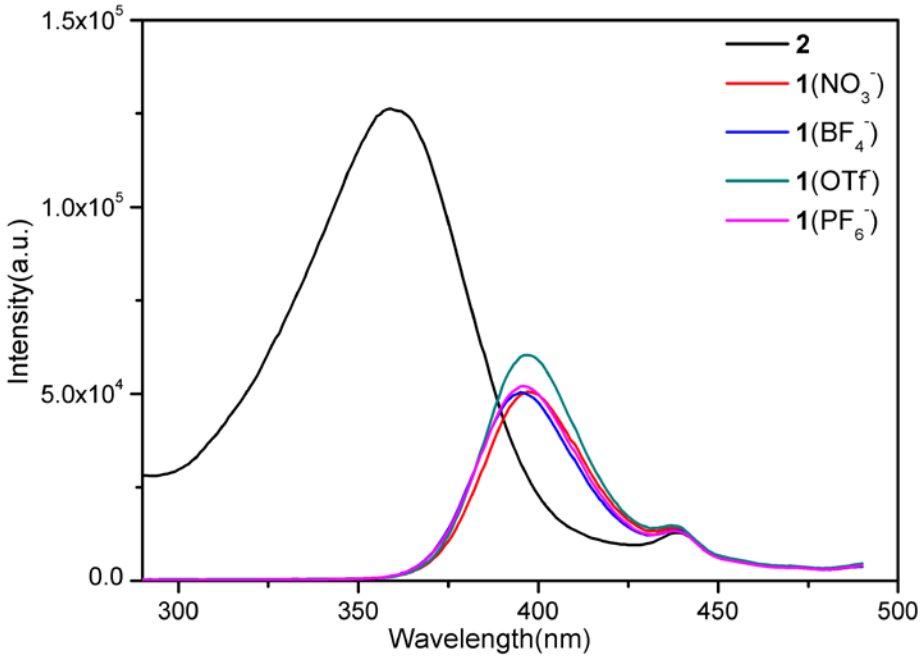

Fig. S15 Excitation spectra of ligand **L** and complexes $Pd_2L_4(NO_3)_4$, $Pd_2L_4(BF_4)_4$, $Pd_2L_4(PF_6)_4$ and $Pd_2L_4(CF_3SO_3)_4$ in DMSO (c = 10^{-4} M, λ_{em} = 500 nm).

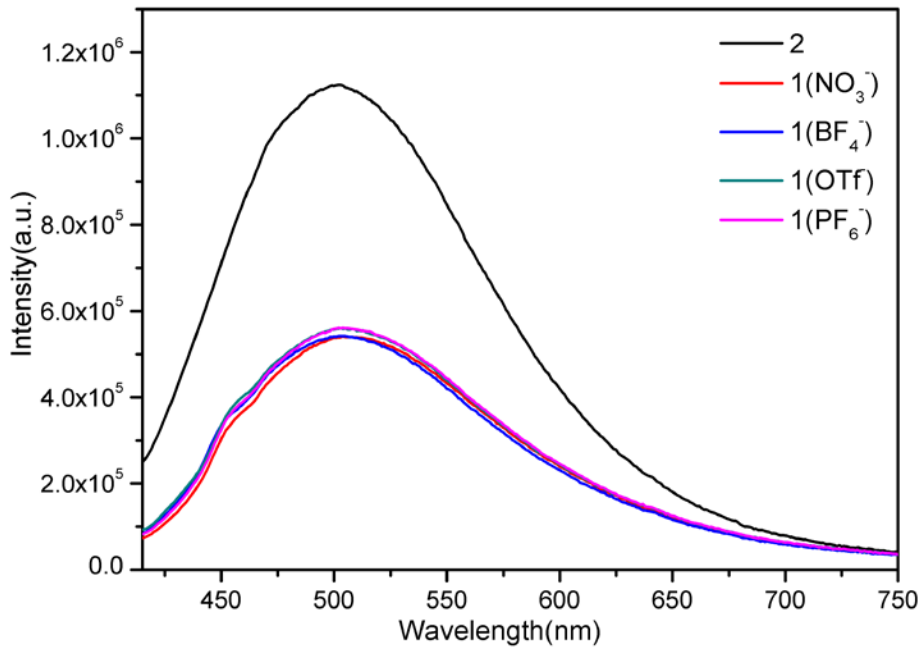

Fig. S16 Fluorescence emission spectra of ligand **L** and complexes $Pd_2L_4(NO_3)_4$, $Pd_2L_4(BF_4)_4$, $Pd_2L_4(PF_6)_4$ and $Pd_2L_4(CF_3SO_3)_4$ in DMSO (c = 10^{-4} M, λ_{ex} = 360, 397,397,397,397nm).

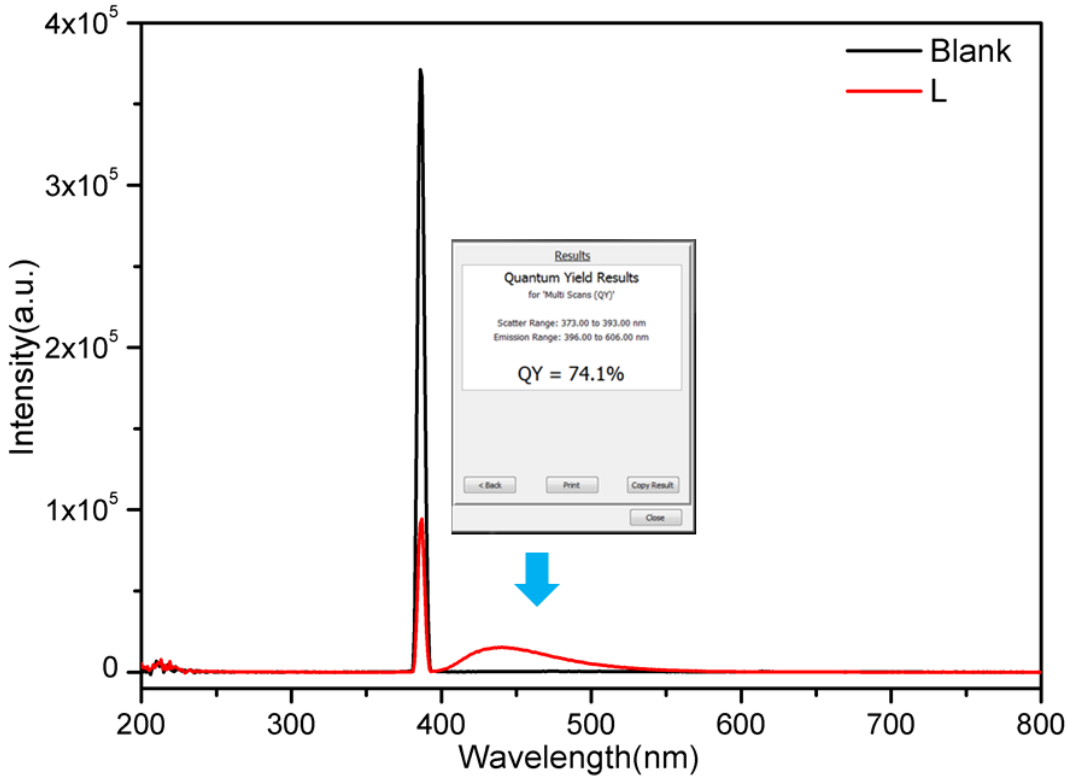

Fig. S17 Quantum yield of **L** in solid state (298K, powder, λex=386nm).

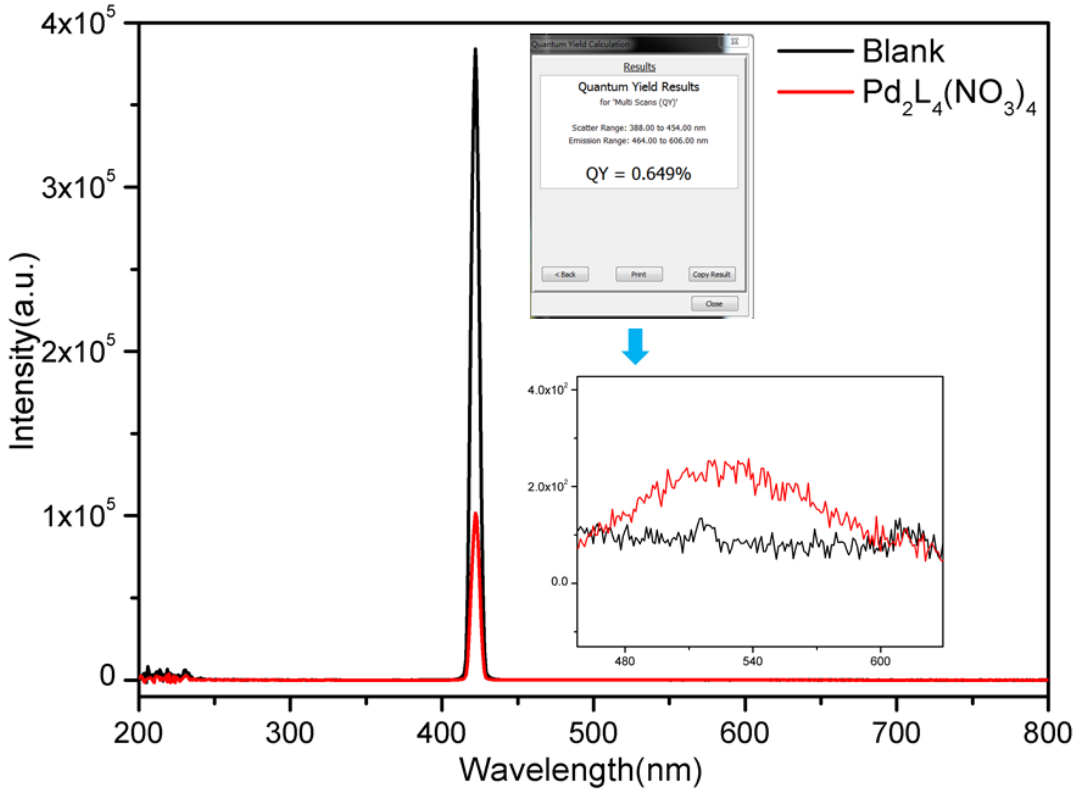

Fig. S18 Quantum yield of $Pd_2L_4(NO_3)_4$ in solid state (298K, powder, λex=420nm).

3.2 The spectra for AIE effect

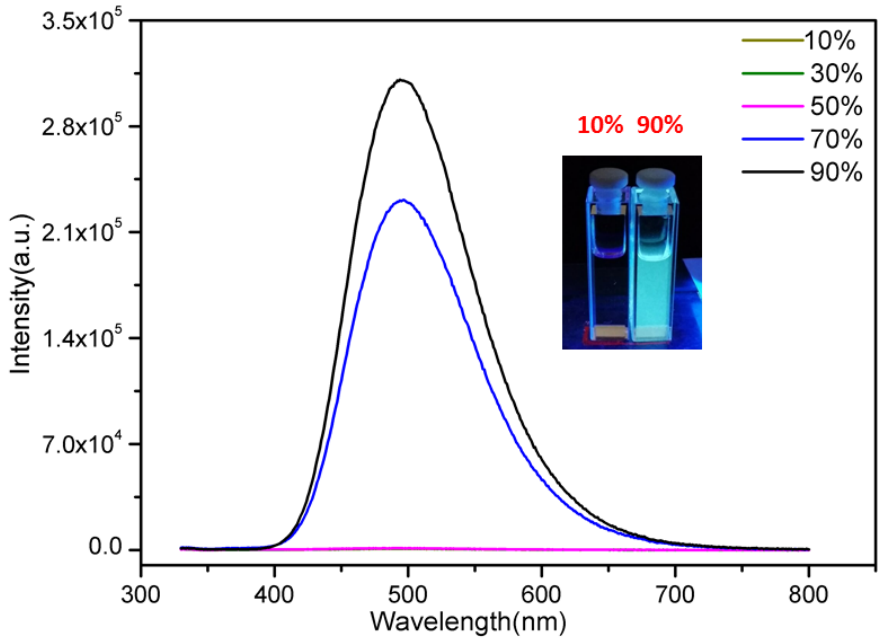

Fig. S19 The photograph and emission spectra of L with increasing H_2O fractions in H_2O/MeOHmixtures (λex = 360nm, c = 1.00 × 10^{-4} M).

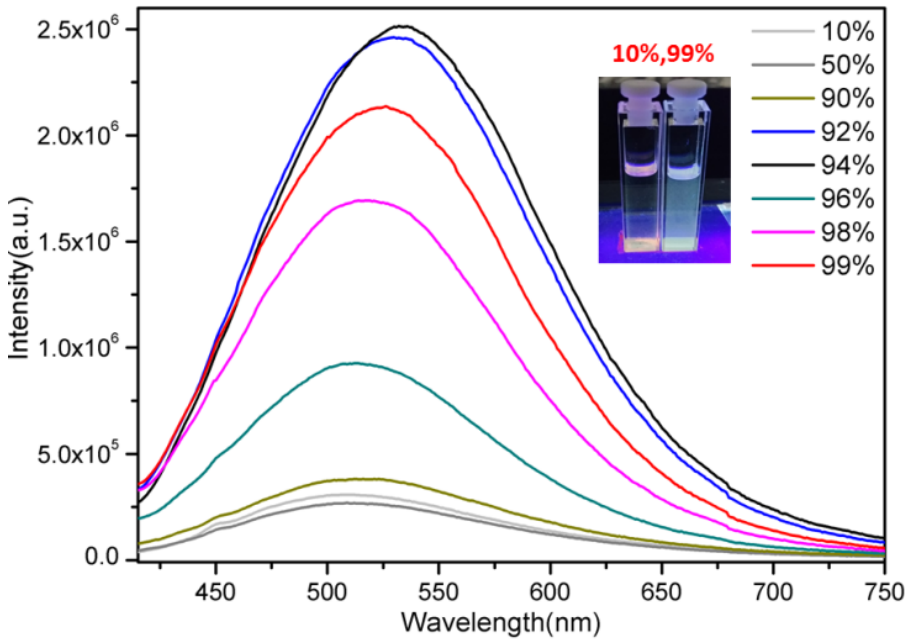

Fig. S20 The photograph and AIE spectra of $Pd_2L_4(NO_3)_4$ with increasing methylbenzene fractions in methylbenzene/DMSO mixtures. (λex = 395nm, c = 1.00 × 10^{-4} M)

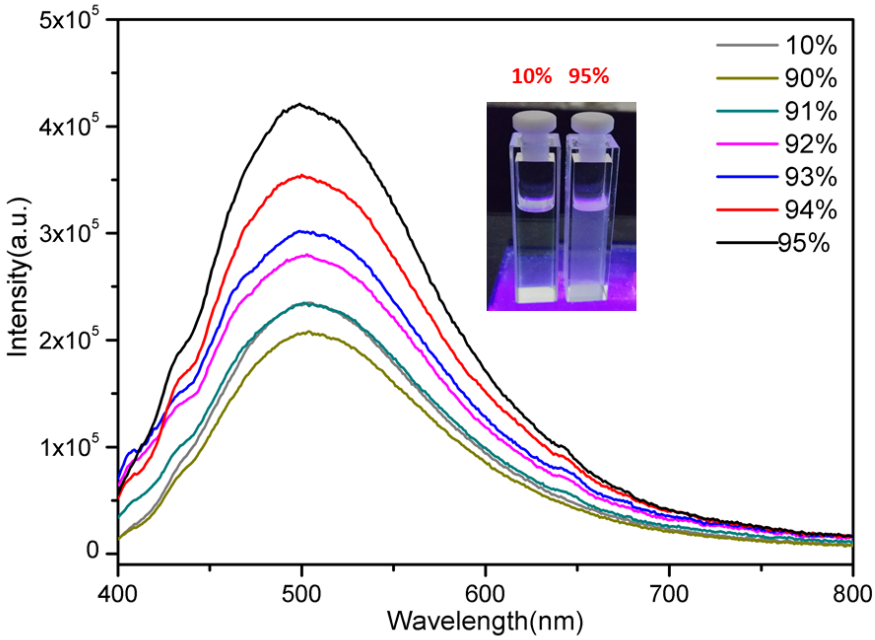

Fig. S21 The photograph and AIE spectra of $Pd_2L_4(NO_3)_4$ with increasing EA fractions in EA/DMSOmixtures. (λex = 395nm, c = 1.00 × 10^{-4} M)

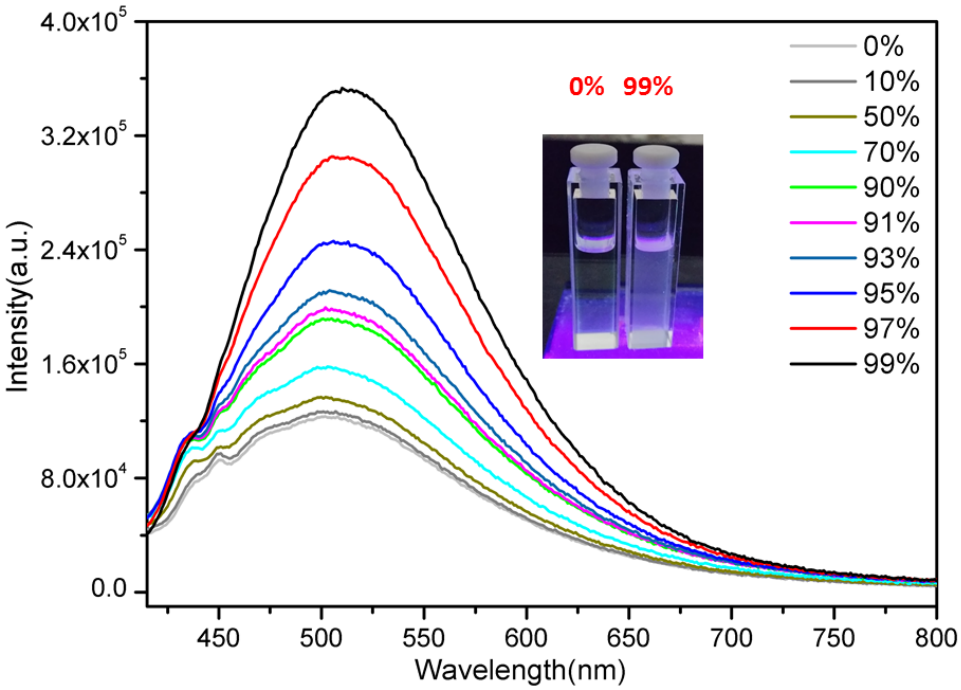

Fig. S22 The photograph and AIE spectra of $Pd_2L_4(NO_3)_4$ with increasing 1,4-dioxane fractions in 1,4-dioxane/DMSO mixtures. (λex = 395nm, c = 1.00 × 10^{-4} M)

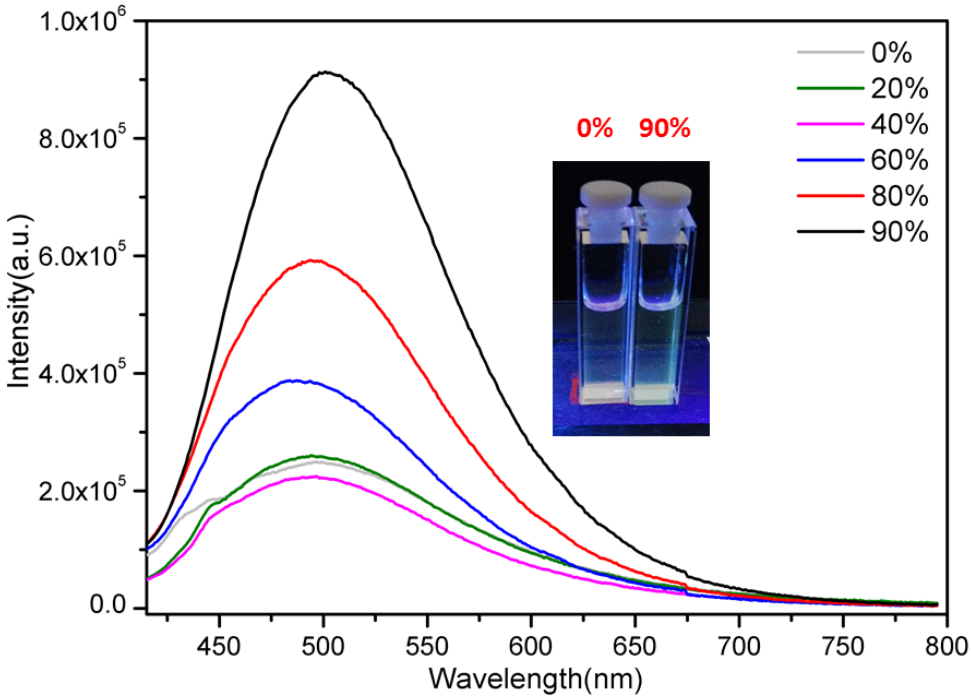

Fig. S23 The photograph and AIE spectra of $Pd_2L_4(NO_3)_4$ with increasing H_2O fractions in H_2O/DMSO mixtures.

(λ ex = 395nm, c = 1.00 × 10^{-4} M)

Elapsed Time	00:03:00
Median Diam.	73.5 nm
Mean Diam.	80.1 nm
Polydispersity	0.206
GSD	1.542

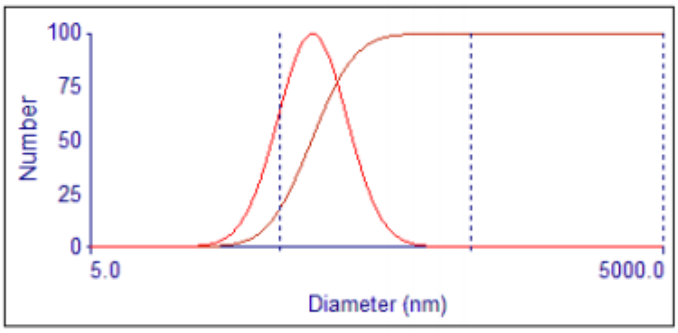

Lognormal Size Distribution

d(nm)	G(d)	C(d)	d(nm)	G(d)	C(d)	d(nm)	G(d)	C(d)
37.3	26	5	66.2	97	40	97.2	80	75
43.3	44	10	69.8	99	45	104.2	70	80
47.9	58	15	73.5	100	50	112.8	58	85
51.9	70	20	77.5	99	55	124.9	44	90
55.7	80	25	81.7	97	60	145.1	26	95
59.2	87	30	86.2	93	65			
62.7	93	35	91.3	87	70			

Fig.S24 Size distributions of L in H_2O/MeOH (3:97 v/v) at $3*10^{-5}$ M by DLS. L showed a hydrodynamic diameter (Dh) of 80.1 nm.

Elapsed Time	00:03:00
Median Diam.	364.2 nm
Mean Diam.	370.0 nm
Polydispersity	0.052
GSD	1.253

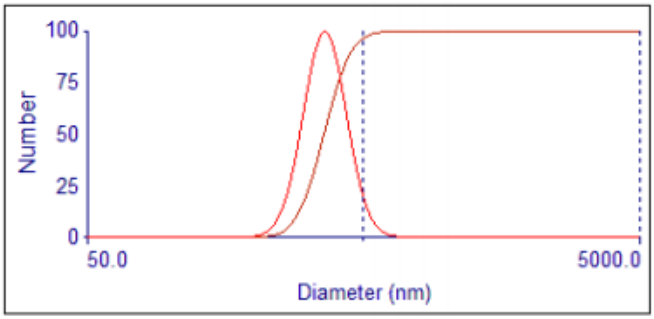

Lognormal Size Distribution

d(nm)	G(d)	C(d)	d(nm)	G(d)	C(d)	d(nm)	G(d)	C(d)
272.0	26	5	348.2	97	40	410.5	80	75
290.1	44	10	356.2	99	45	423.0	70	80
303.0	58	15	364.2	100	50	437.8	58	85
313.7	70	20	372.5	99	55	457.3	44	90
323.2	80	25	381.0	97	60	487.8	26	95
331.9	87	30	390.0	93	65			
340.2	93	35	399.8	87	70			

Fig. S25 Size distributions of $Pd_2L_4(NO_3)_4$ in methylbenzene /DMSO (1:99 v/v) at 10^{-4} M by DLS. $Pd_2L_4(NO_3)_4$ showed a hydrodynamic diameter (Dh) of 370 nm.

3.3 The spectra for EIE

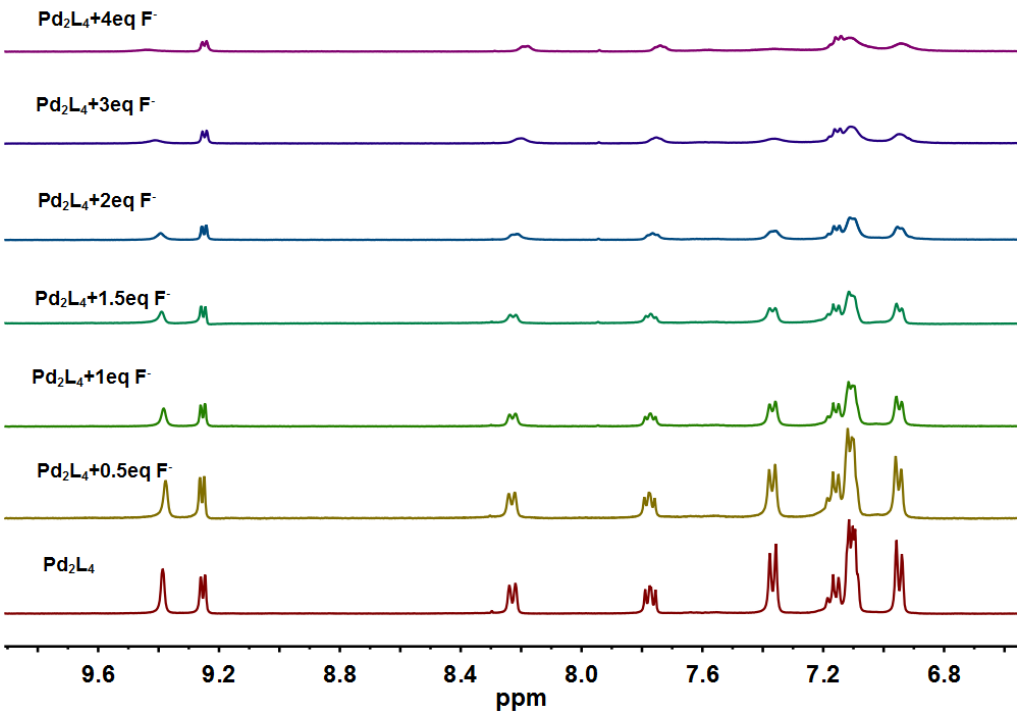

Fig. S26 ^{1}H NMR spectra of $Pd_2L_4(CF_3SO_3)_4$ with the addition of different equiv of $N(C_4H_9)_4F$ (400 MHz, [D_6]DMSO, 298K)

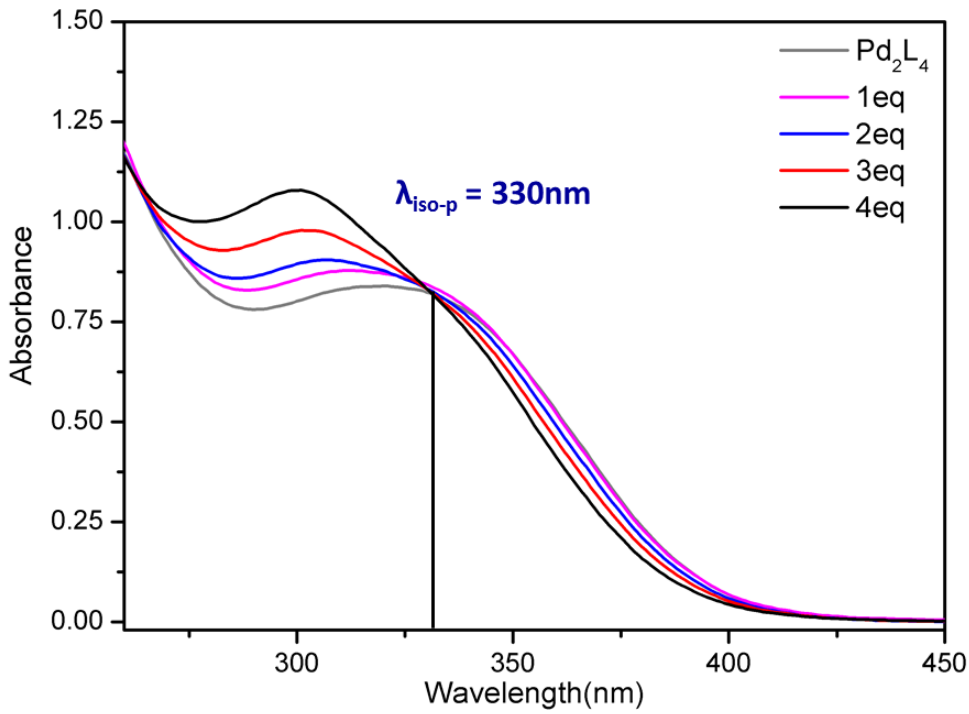

Fig. S27 UV-vis absorption spectra of $Pd_2L_4(CF_3SO_3)_4$ with the addition of different equiv of $N(C_4H_9)_4F$ (c = 1.0 × 10^{-5} M)

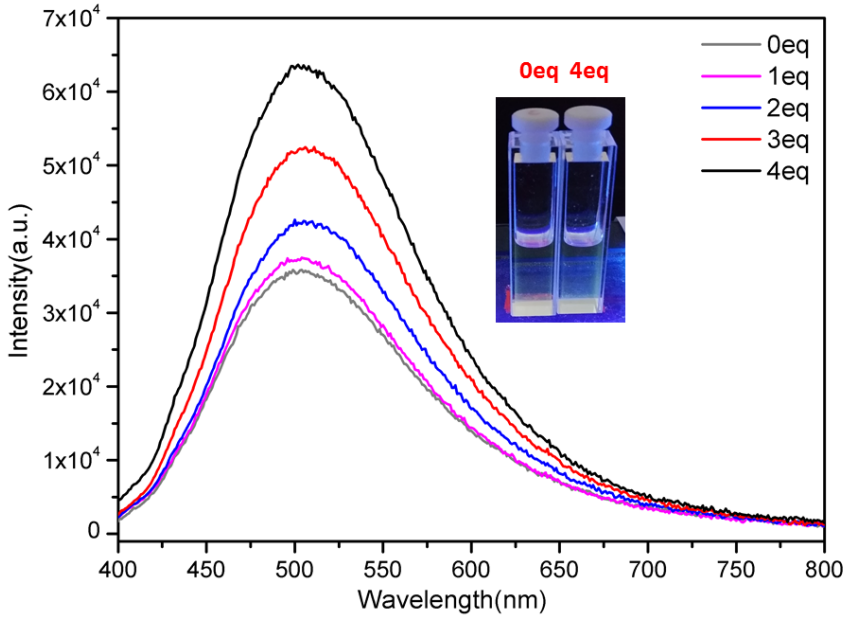

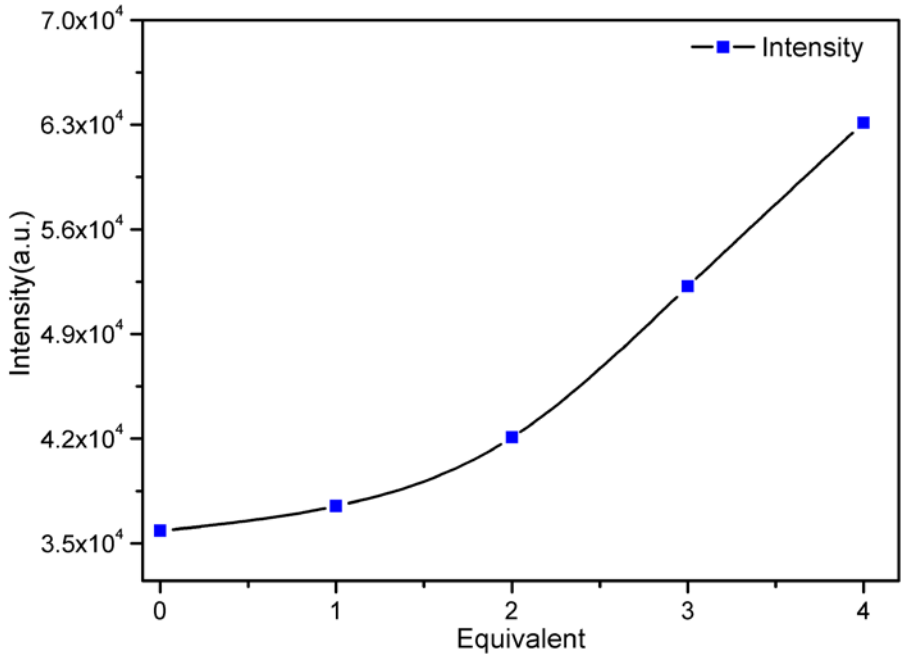

Fig. S28 Fluorescence titration spectra of $Pd_2L_4(CF_3SO_3)_4$ with the addition of different equiv of $N(C_4H_9)_4F$ (c =1.0 × 10^{-4} M, λ_{ex} = 380 nm).

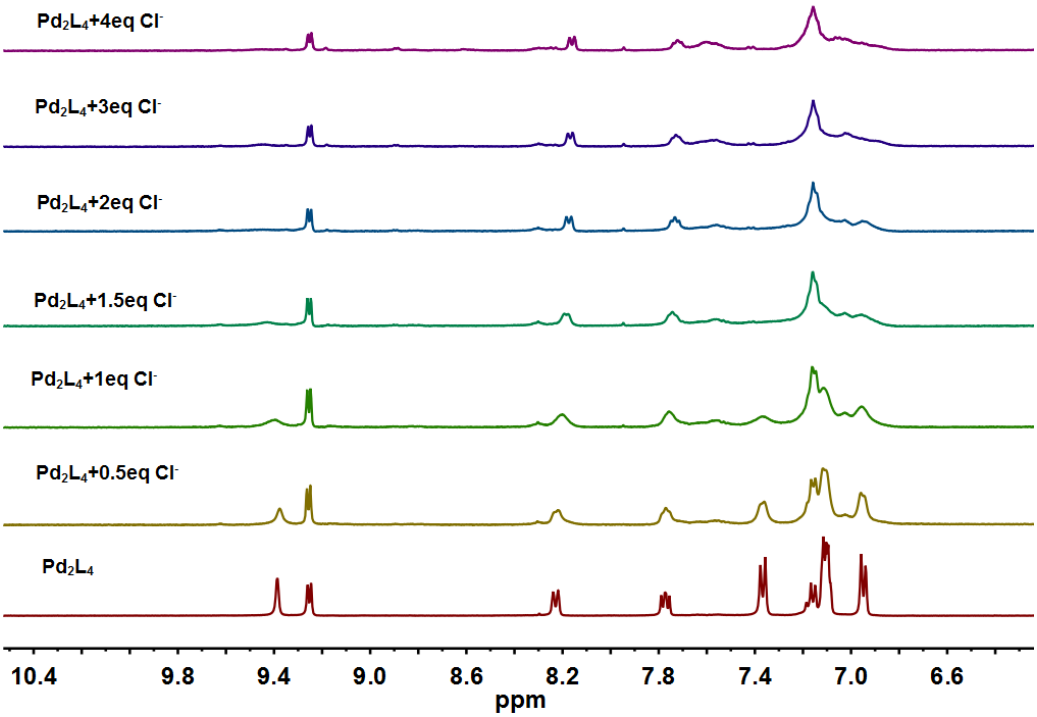

Fig. S29 ^{1}H NMR spectra of $Pd_2L_4(CF_3SO_3)_4$ with the addition of different equiv of $N(C_4H_9)_4Cl$ (400 MHz, [D_6]DMSO, 298K)

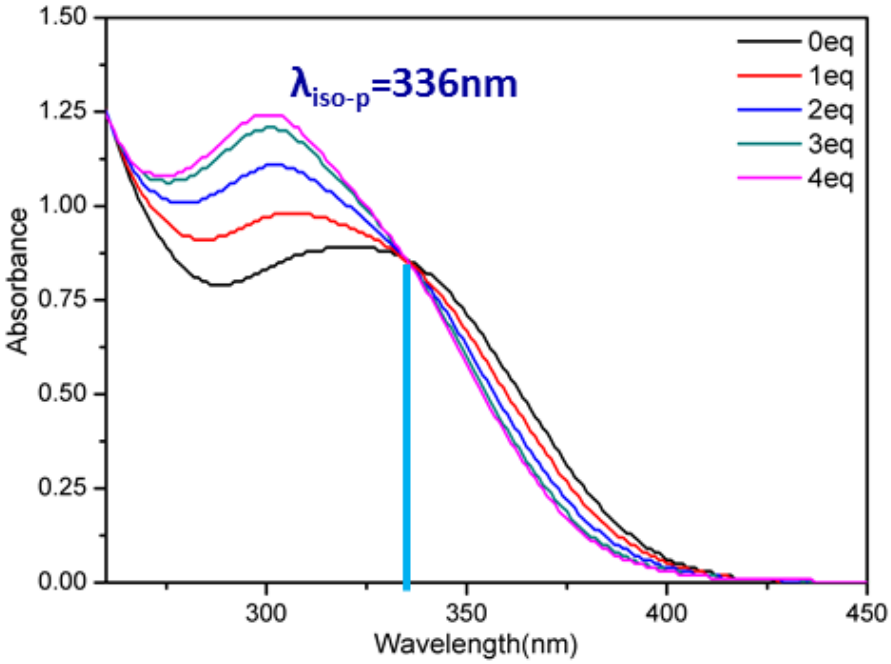

Fig. S30 UV-vis absorption spectra of $Pd_2L_4(CF_3SO_3)_4$ with the addition of different equiv of $N(C_4H_9)_4Cl$ (c = 1.0 × 10^{-5} M)

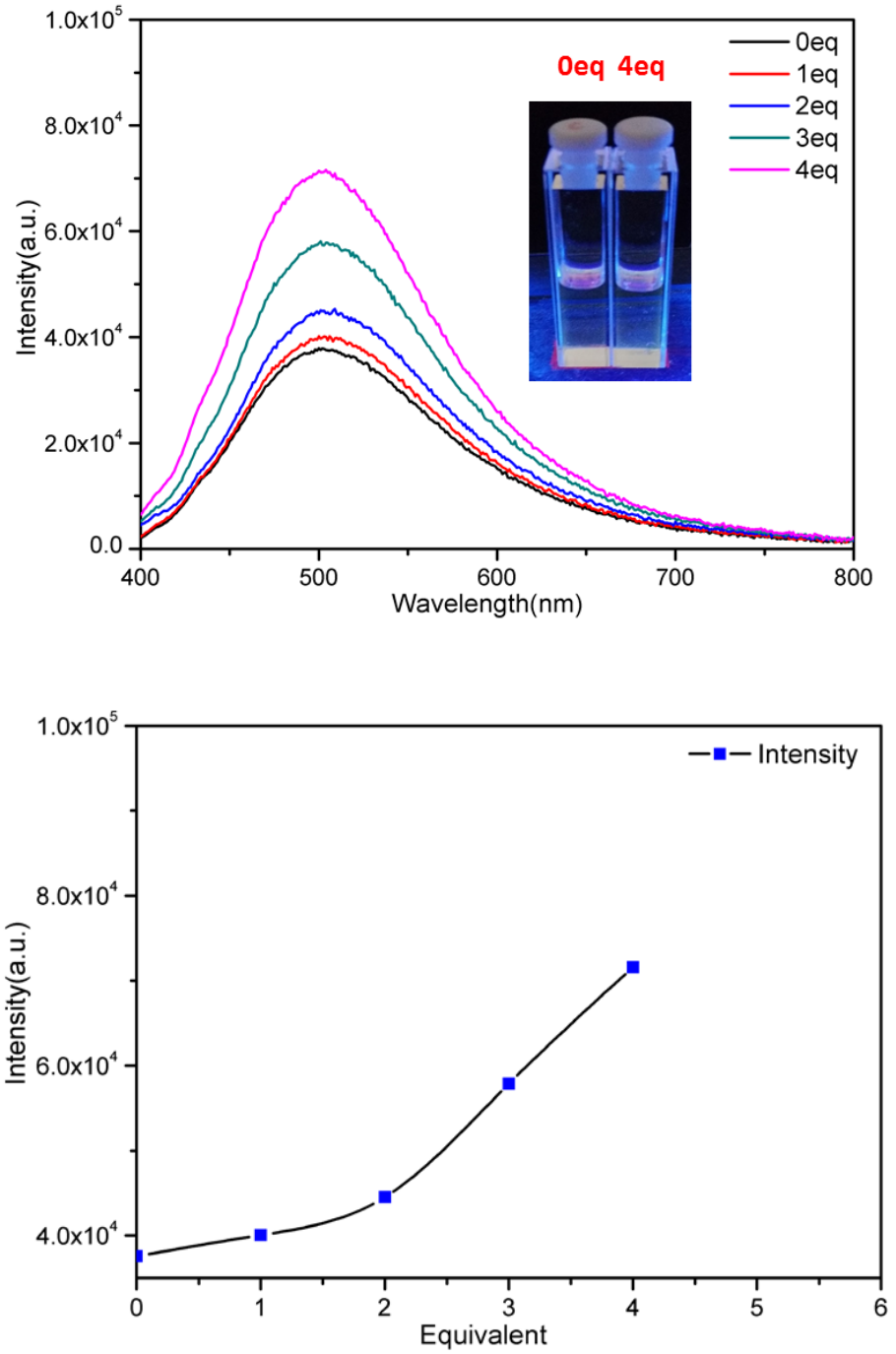

Fig. S31 Fluorescence titration spectra of $Pd_2L_4(CF_3SO_3)_4$ with the addition of different equiv of $N(C_4H_9)_4Cl$ (1.0 × 10^{-4}M, λ_{ex} = 380 nm).

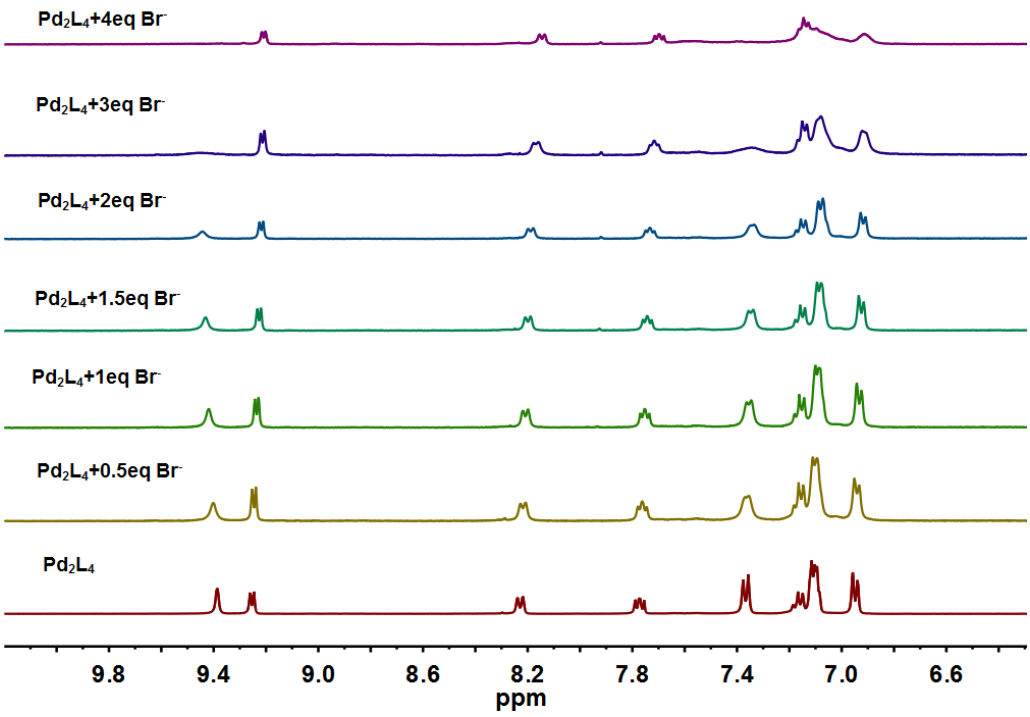

Fig. S32 ^{1}H NMR spectra of $Pd_2L_4(CF_3SO_3)_4$ with the addition of different equiv of $N(C_4H_9)_4Br$ (400 MHz, [D_6]DMSO, 298K)

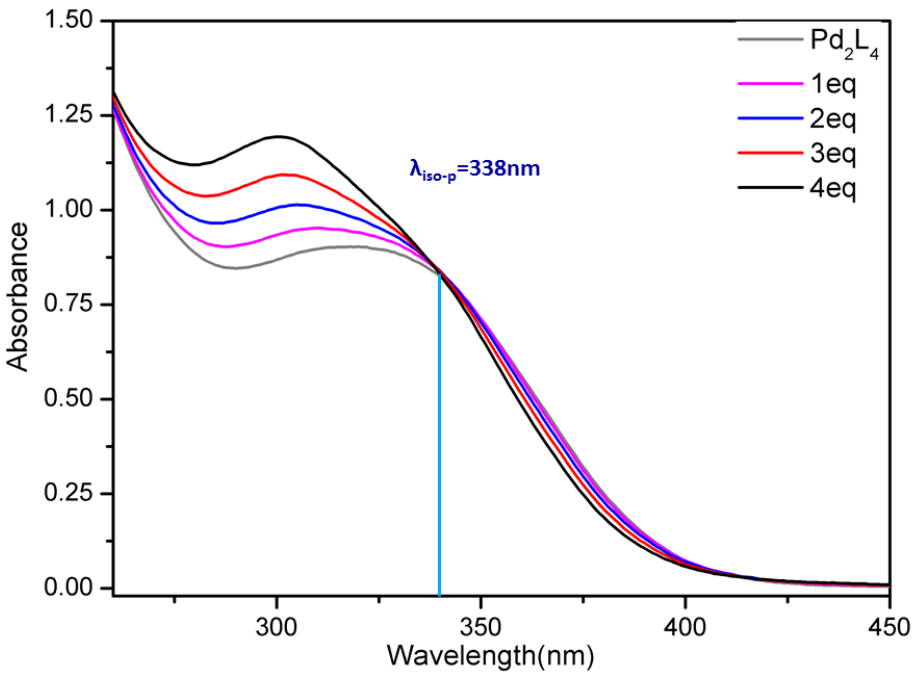

Fig. S33 UV-vis absorption spectra of $Pd_2L_4(CF_3SO_3)_4$ with the addition of different equiv of $N(C_4H_9)_4Br$ (c = 1.0 × 10^{-5} M)

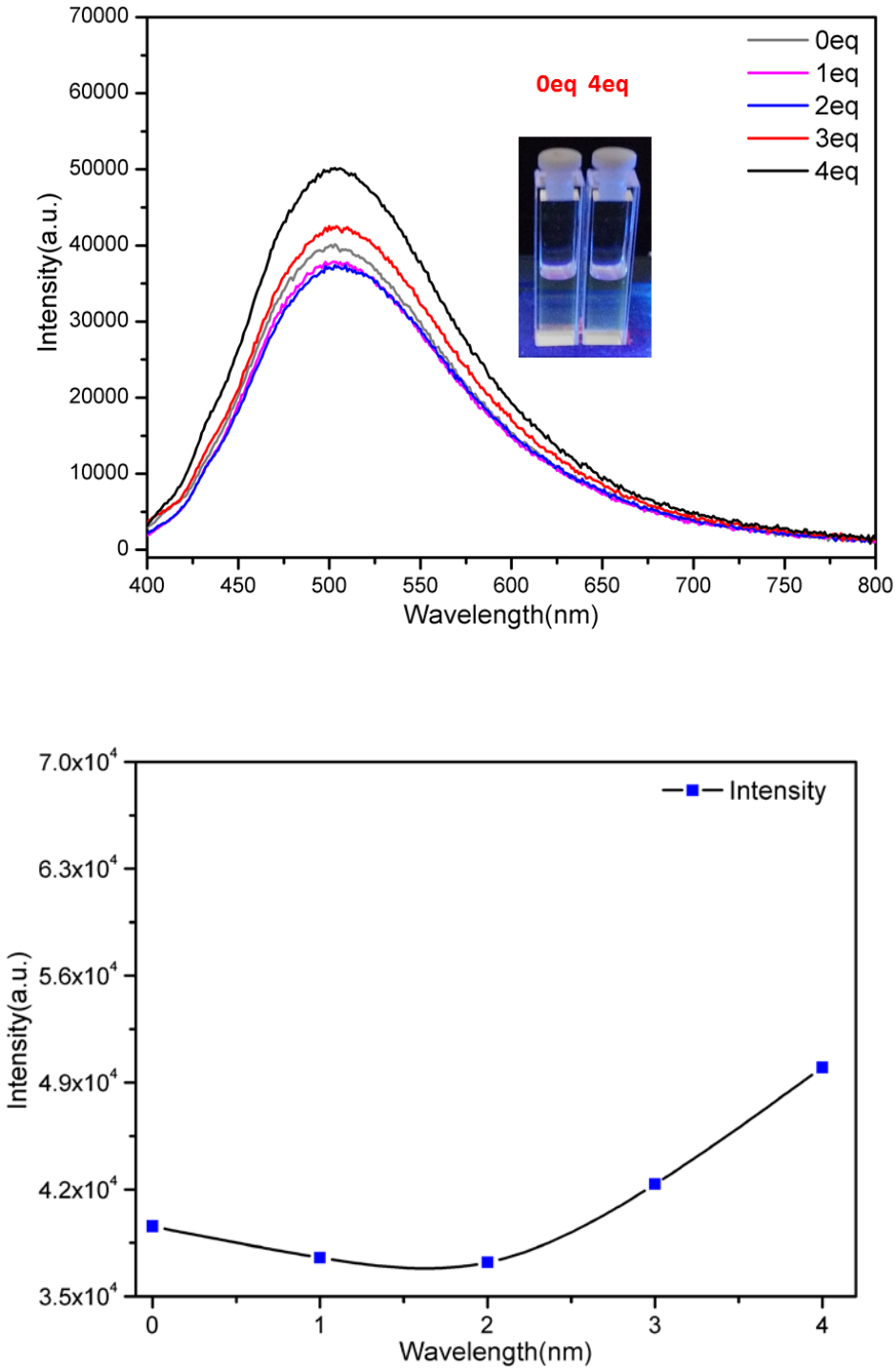

Fig. S34 Fluorescence titration spectra of $Pd_2L_4(CF_3SO_3)_4$ with the addition of different equiv of $N(C_4H_9)_4Br$ (1.0 × 10^{-4} M, λ_{ex} = 380 nm).

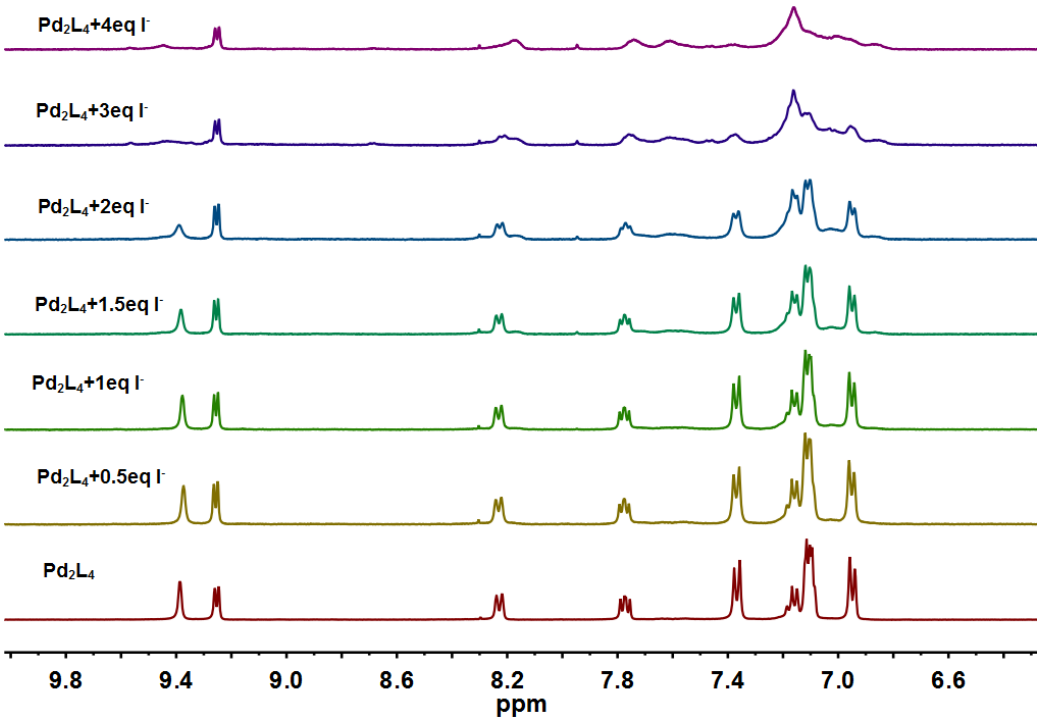

Fig. S35 ^{1}H NMR spectra of $Pd_2L_4(CF_3SO_3)_4$ with the addition of different equiv of $N(C_4H_9)_4I$ (400 MHz, [D_6]DMSO, 298K)

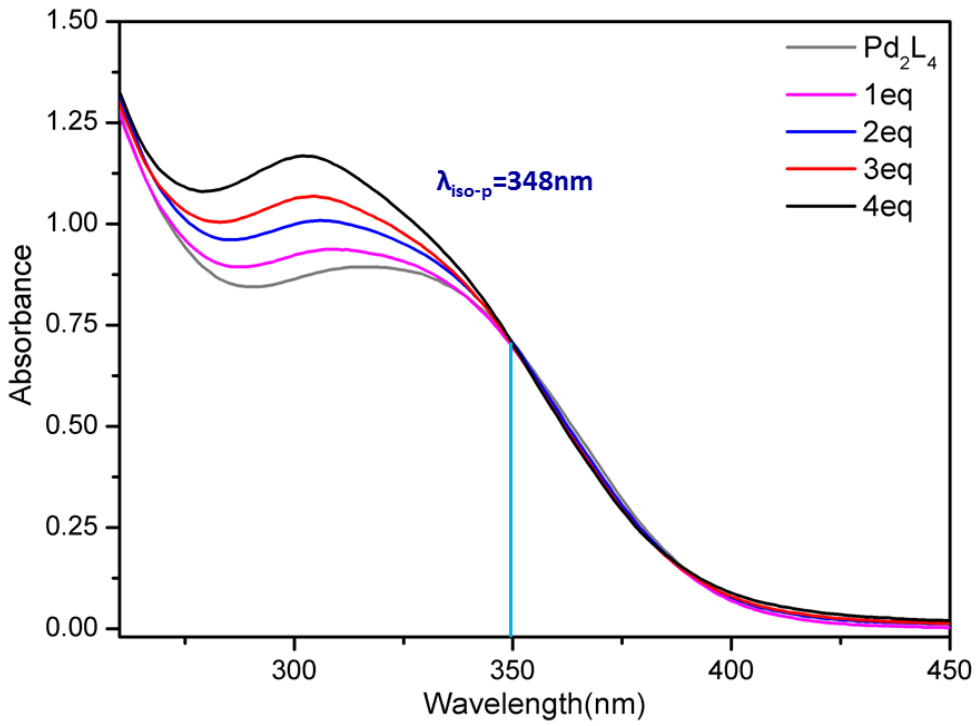

Fig. S36 UV-vis absorption spectra of $Pd_2L_4(CF_3SO_3)_4$ with the addition of different equiv of $N(C_4H_9)_4I$ (c = 1.0 × 10^{-5} M)

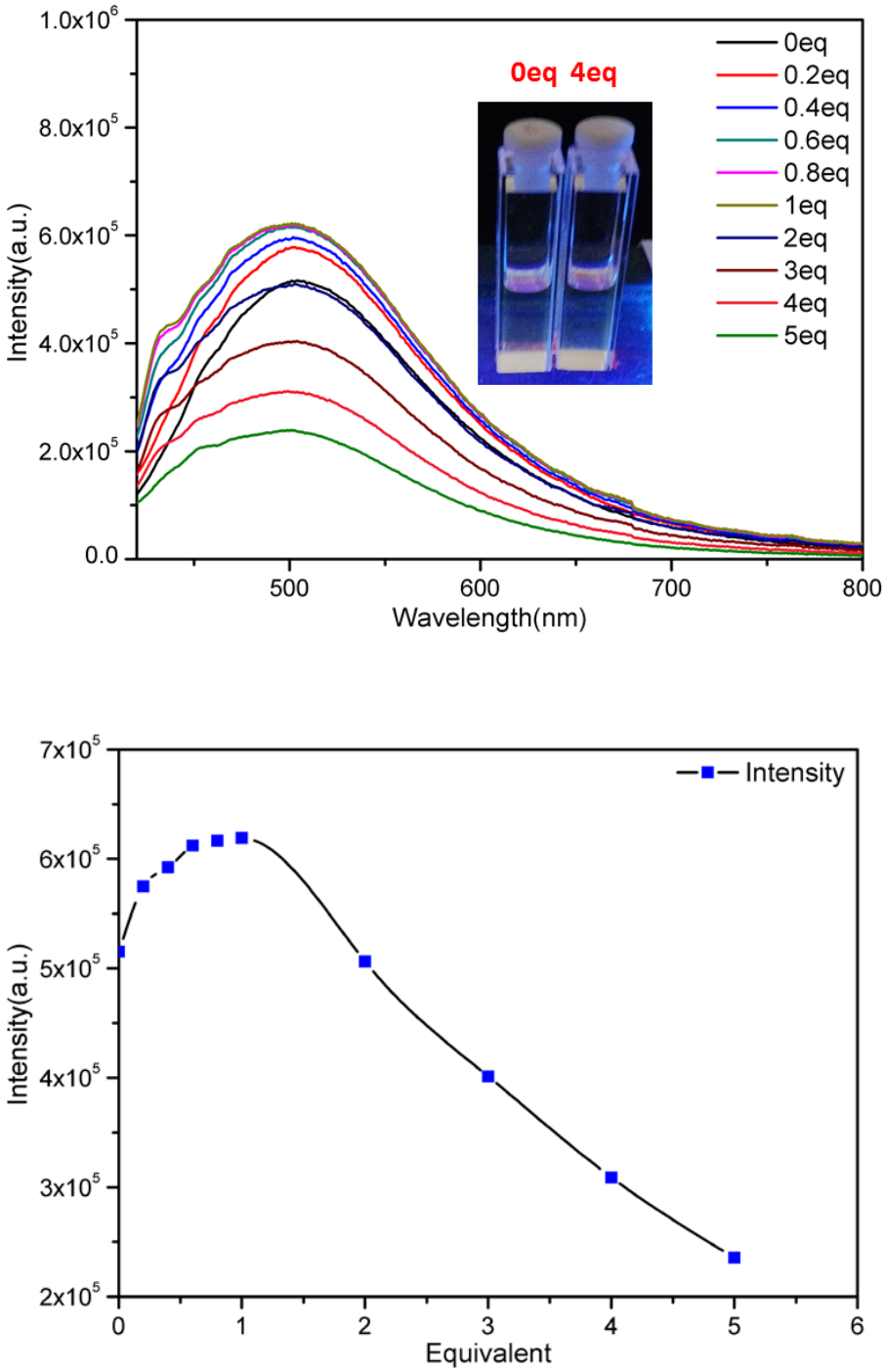

Fig. S37 Fluorescence titration spectra of $Pd_2L_4(CF_3SO_3)_4$ with the addition of different equiv of $N(C_4H_9)_4I$ (1.0×10^{-4} M, λ_{ex} = 380 nm).

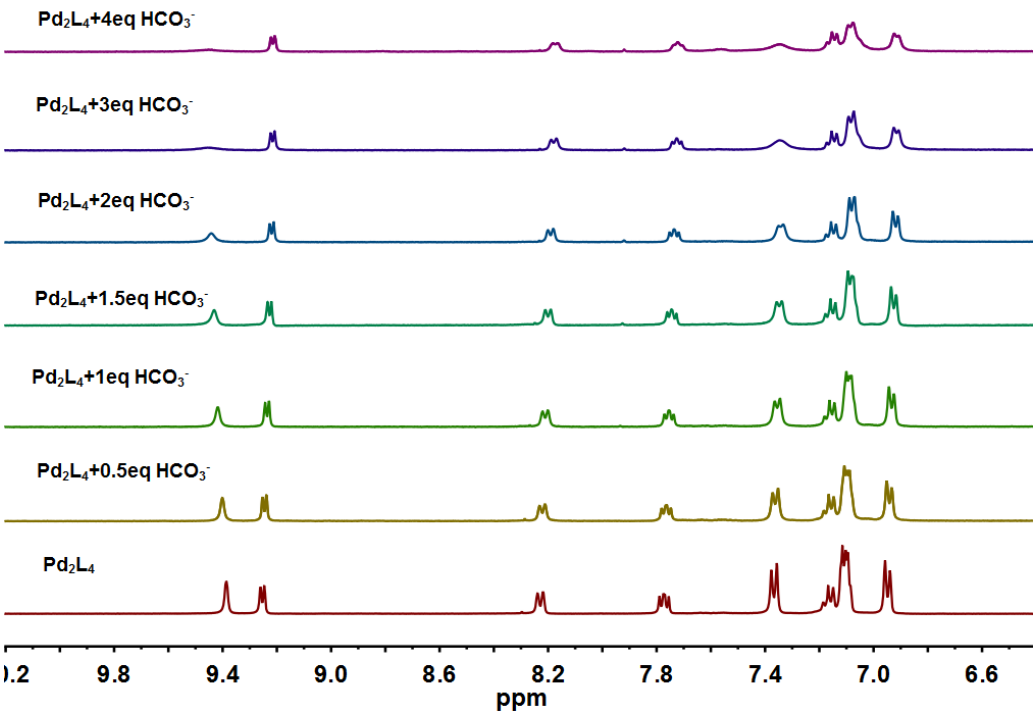

Fig. S38 ^{1}H NMR spectra of $Pd_2L_4(CF_3SO_3)_4$ with the addition of different equiv of $N(C_4H_9)_4HCO_3$ (400 MHz, [D_6]DMSO, 298K)

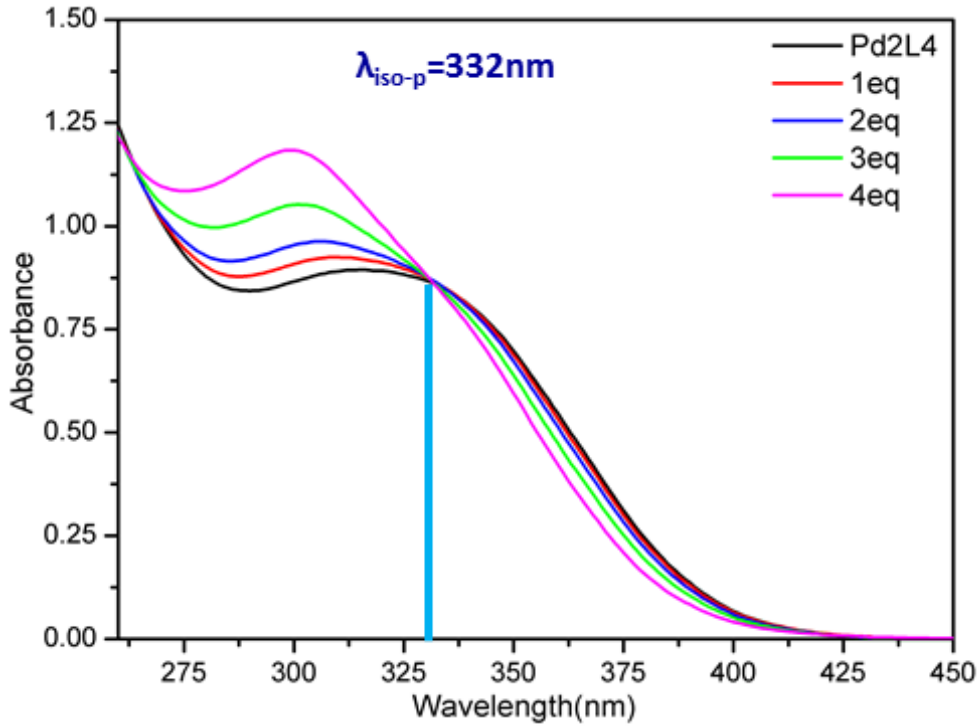

Fig. S39 UV-vis absorption spectra of $Pd_2L_4(CF_3SO_3)_4$ with the addition of different equiv of $N(C_4H_9)_4HCO_3$ (c = 1.0×10^{-5} M)

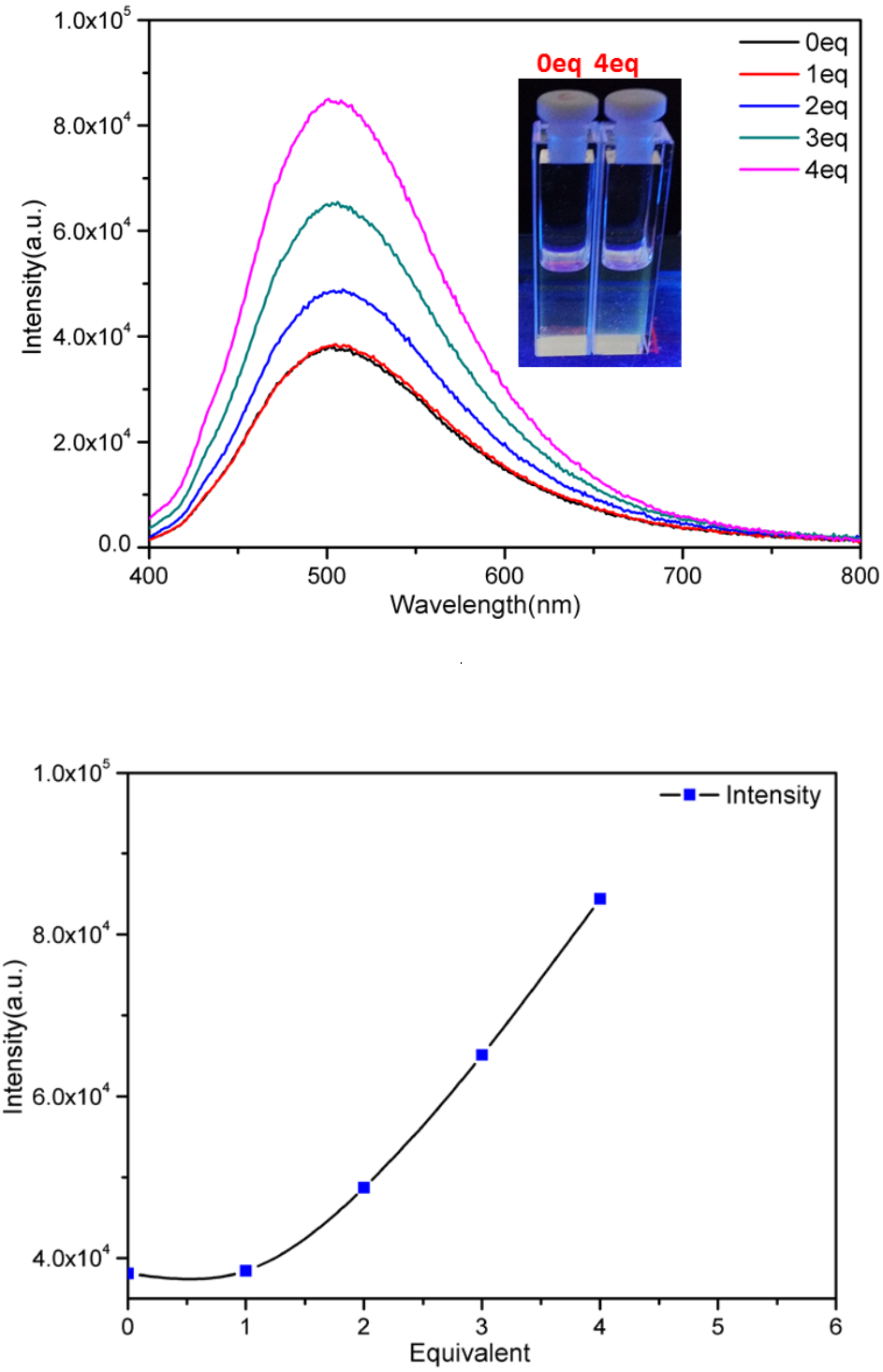

Fig. S40 Fluorescence titration spectra of $Pd_2L_4(CF_3SO_3)_4$ with the addition of different equiv of $N(C_4H_9)_4HCO_3$ (1.0×10^{-4} M, λ_{ex} = 380 nm).

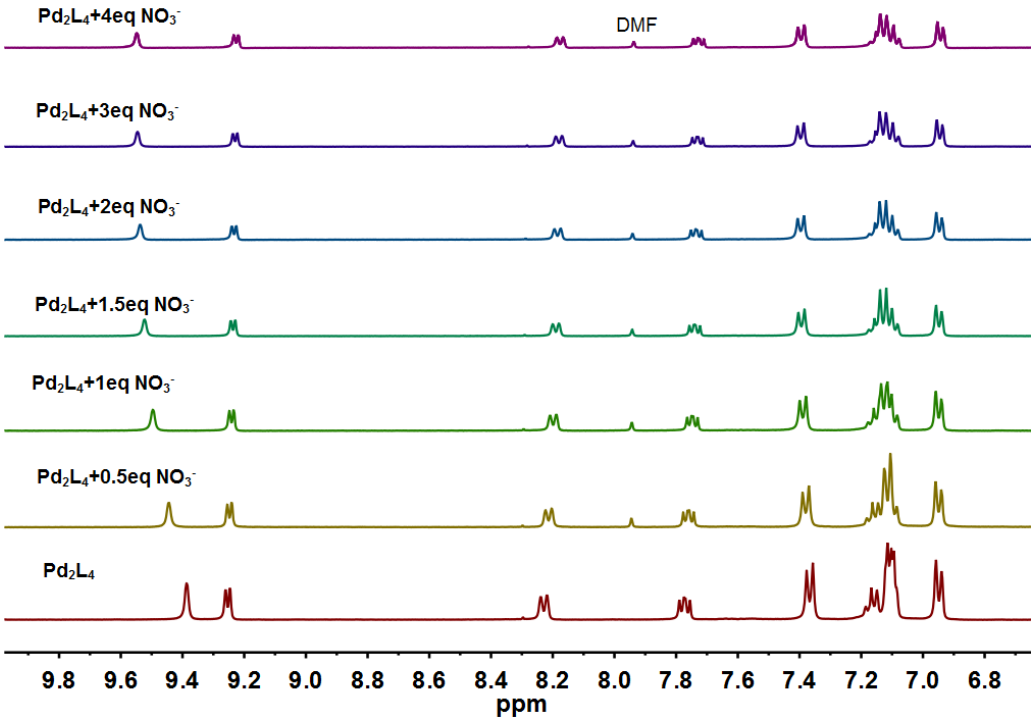

Fig. S41 ^{1}H NMR spectra of $Pd_2L_4(CF_3SO_3)_4$ with the addition of different equiv of $N(C_4H_9)_4NO_3$ (400 MHz, [D_6]DMSO, 298K)

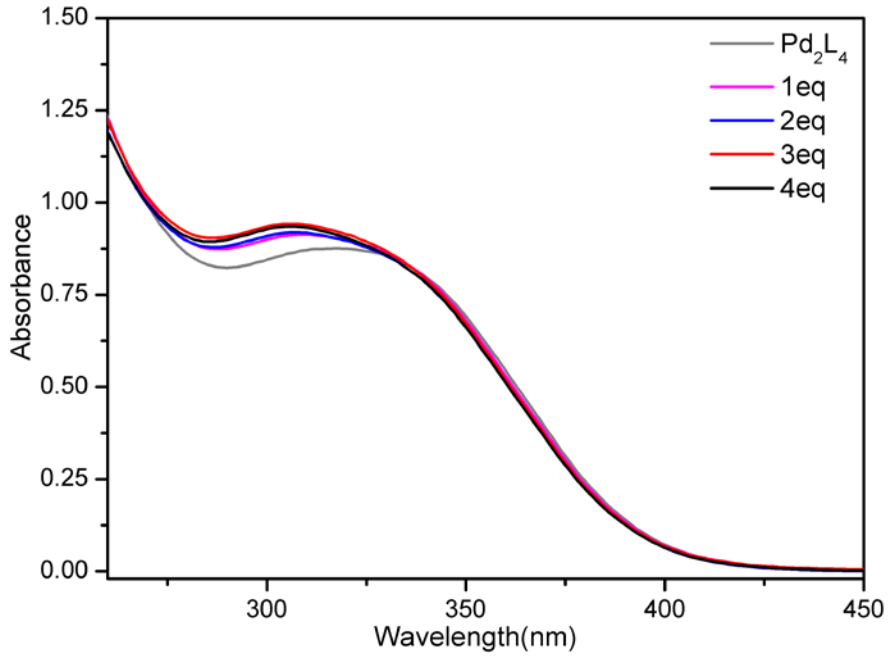

Fig. S42 UV-vis absorption spectra of $Pd_2L_4(CF_3SO_3)_4$ with the addition of different equiv of $N(C_4H_9)_4NO_3$ (c = 1.0×10^{-5} M)

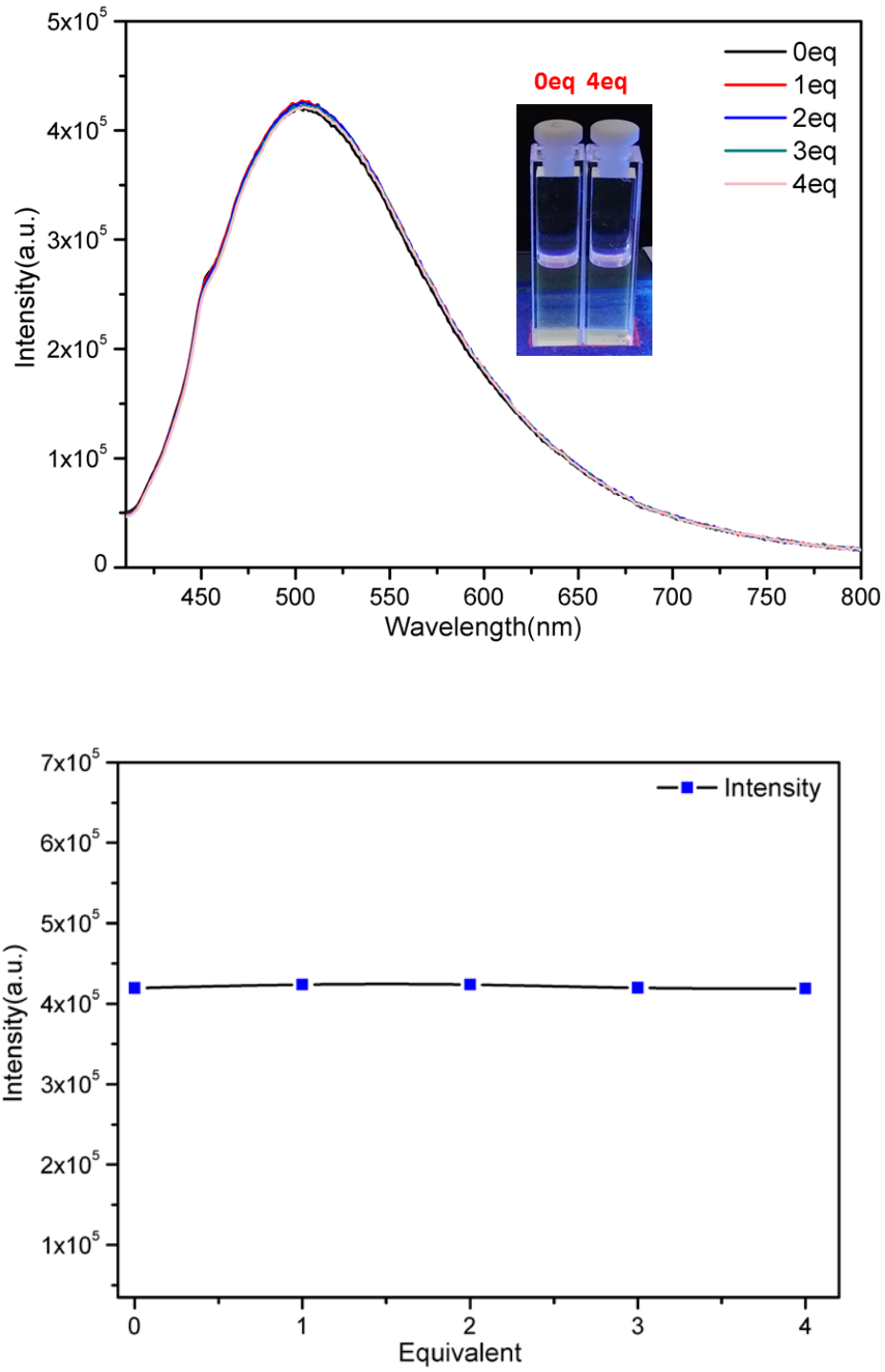

Fig. S43 Fluorescence titration spectra of $Pd_2L_4(CF_3SO_3)_4$ with the addition of different equiv of $N(C_4H_9)_4NO_3$ (1.0×10^{-4} M, λ_{ex} = 380 nm).

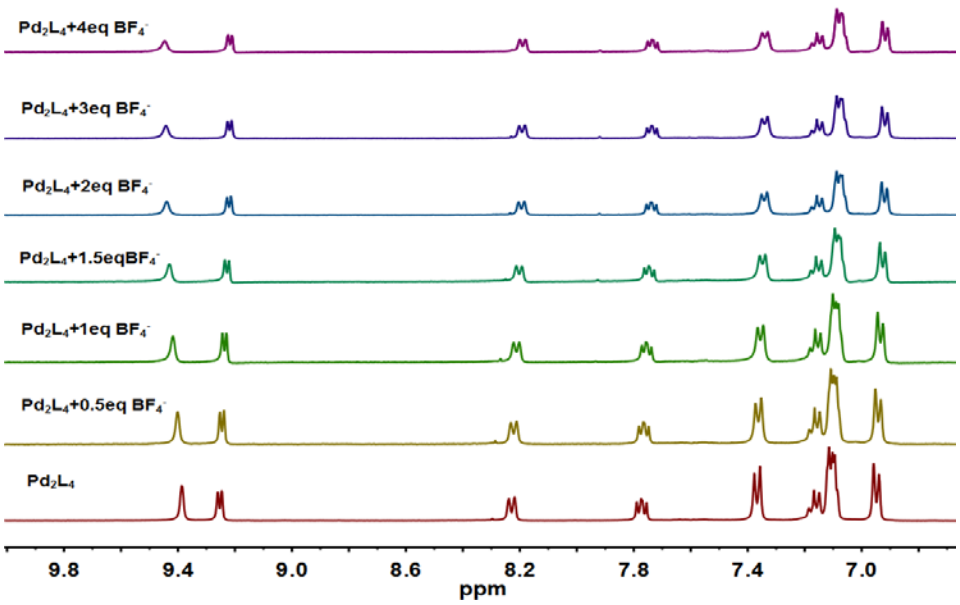

Fig. S44 ^{1}H NMR spectra of $Pd_2L_4(CF_3SO_3)_4$ with the addition of different equiv of $N(C_4H_9)_4BF_4$ (400 MHz, [D_6]DMSO, 298K)

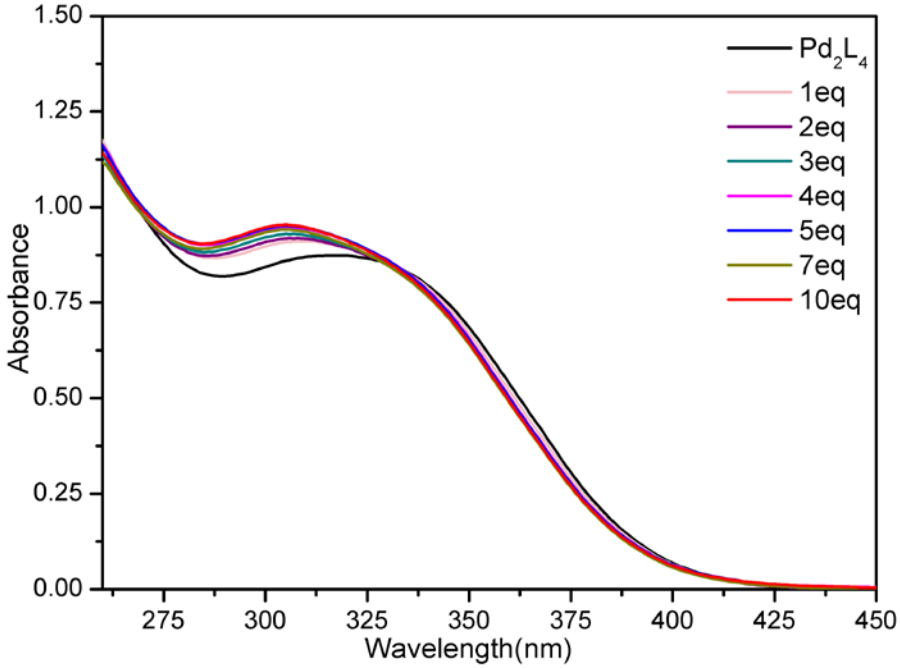

Fig. S45 UV-vis absorption spectra of $Pd_2L_4(CF_3SO_3)_4$ with the addition of different equiv of $N(C_4H_9)_4BF_4$ (c = 1.0 × 10^{-5} M)

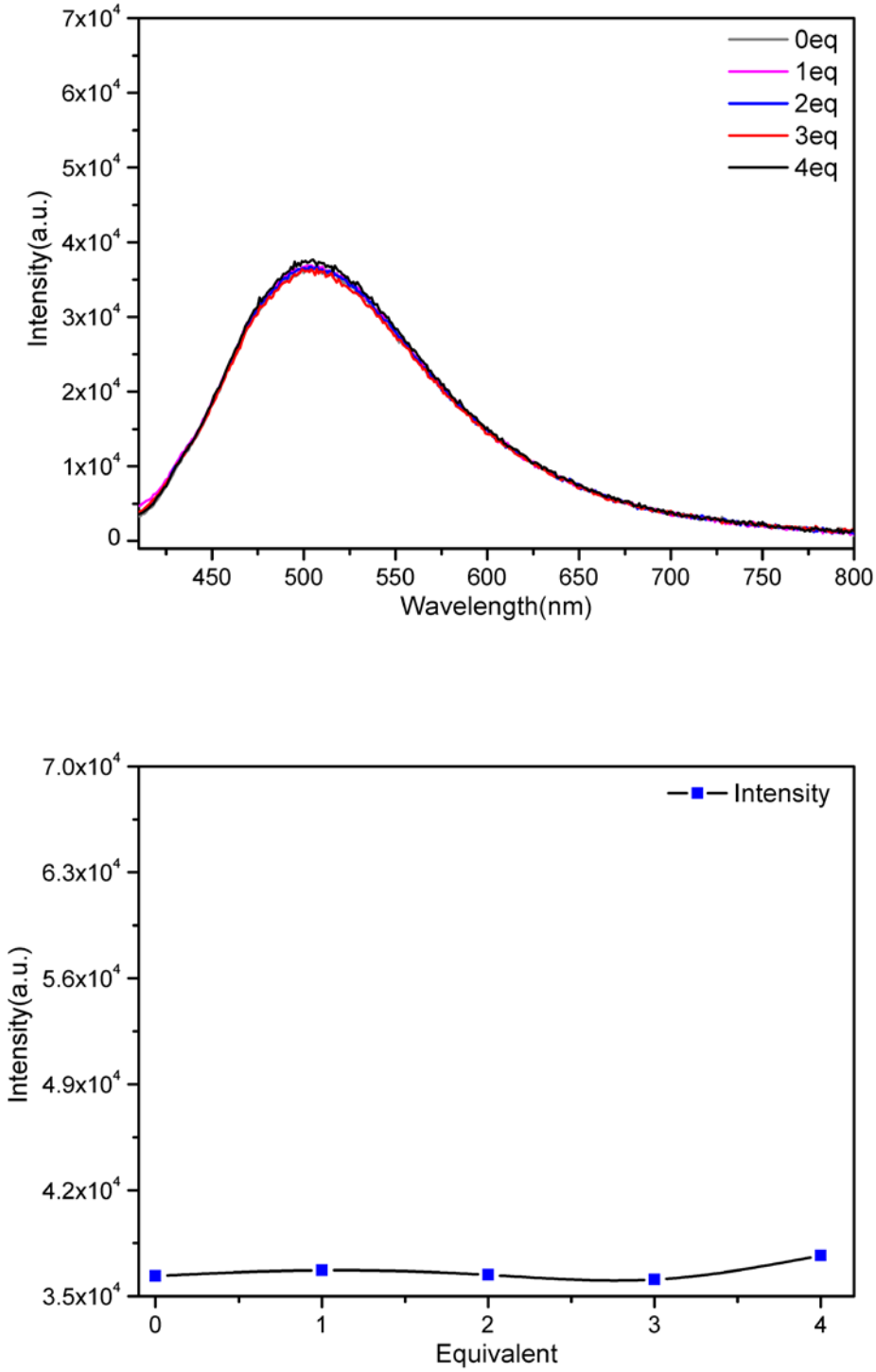

Fig. S46 Fluorescence titration spectra of $Pd_2L_4(CF_3SO_3)_4$ with the addition of different equiv of $N(C_4H_9)_4BF_4$ (1.0 × 10^{-4} M, λ_{ex} = 380 nm).

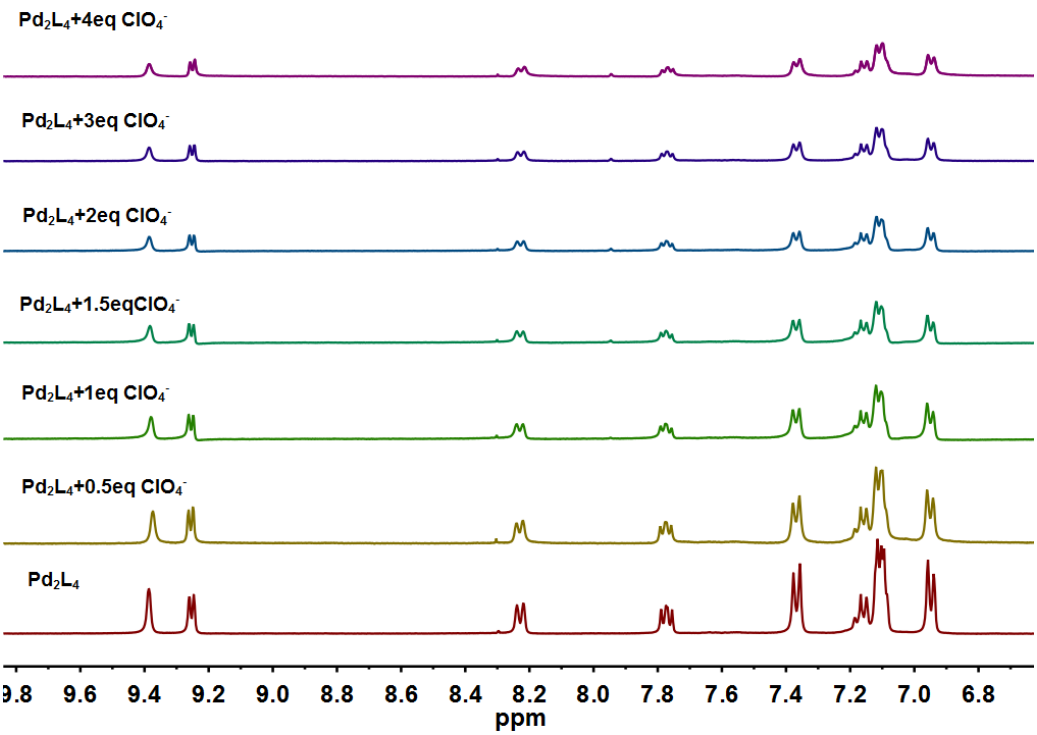

Fig. S47 ^{1}H NMR spectra of $Pd_2L_4(CF_3SO_3)_4$ with the addition of different equiv of $N(C_4H_9)_4ClO_4$ (400 MHz, [D_6]DMSO, 298K)

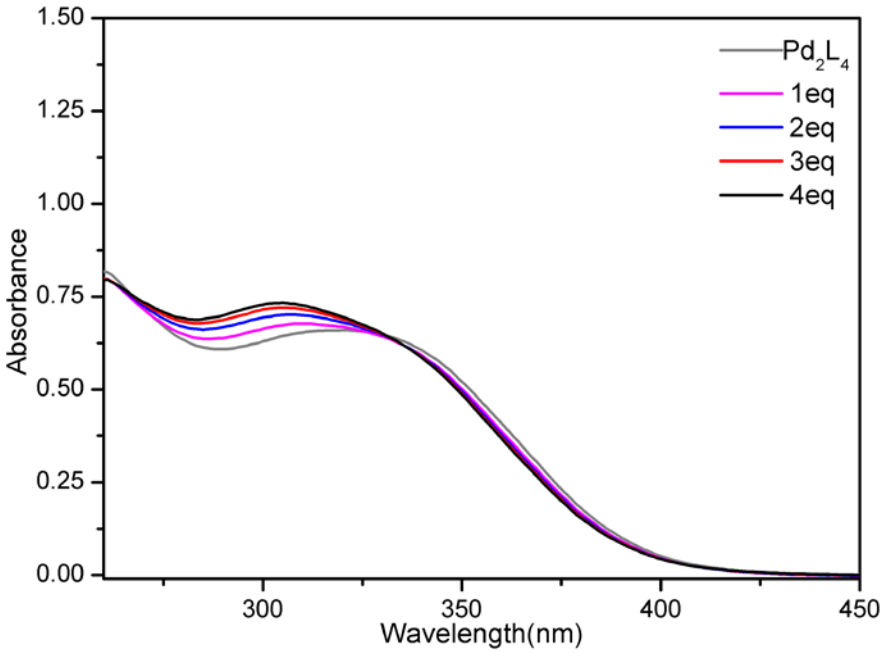

Fig. S48 UV-vis absorption spectra of $Pd_2L_4(CF_3SO_3)_4$ with the addition of different equiv of $N(C_4H_9)_4ClO_4$ (c = 1.0×10^{-5} M)

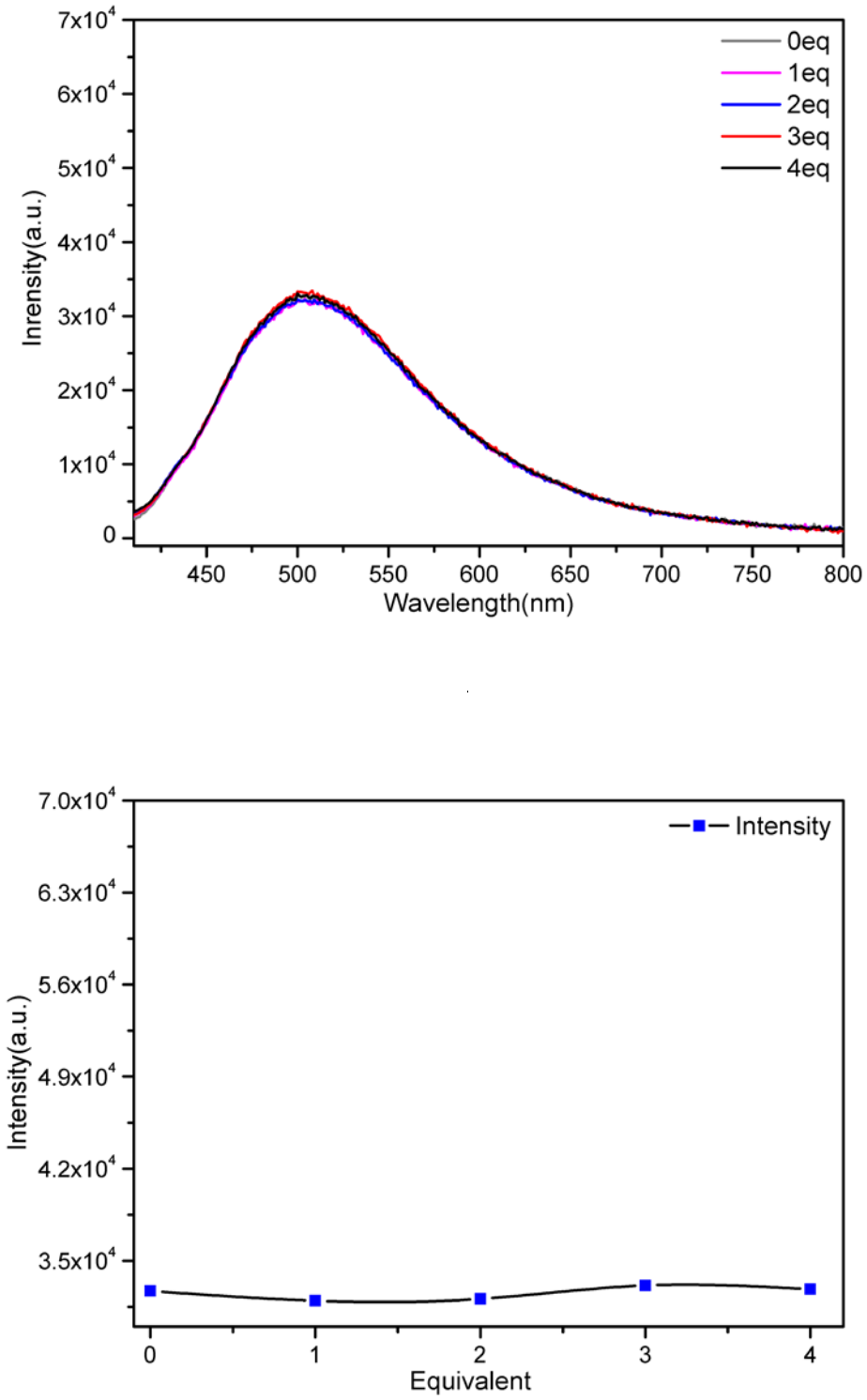

Fig. S49 Fluorescence titration spectra of $Pd_2L_4(CF_3SO_3)_4$ with the addition of different equiv of $N(C_4H_9)_4ClO_4$ (1.0×10^{-4} M, λ_{ex} = 380 nm).

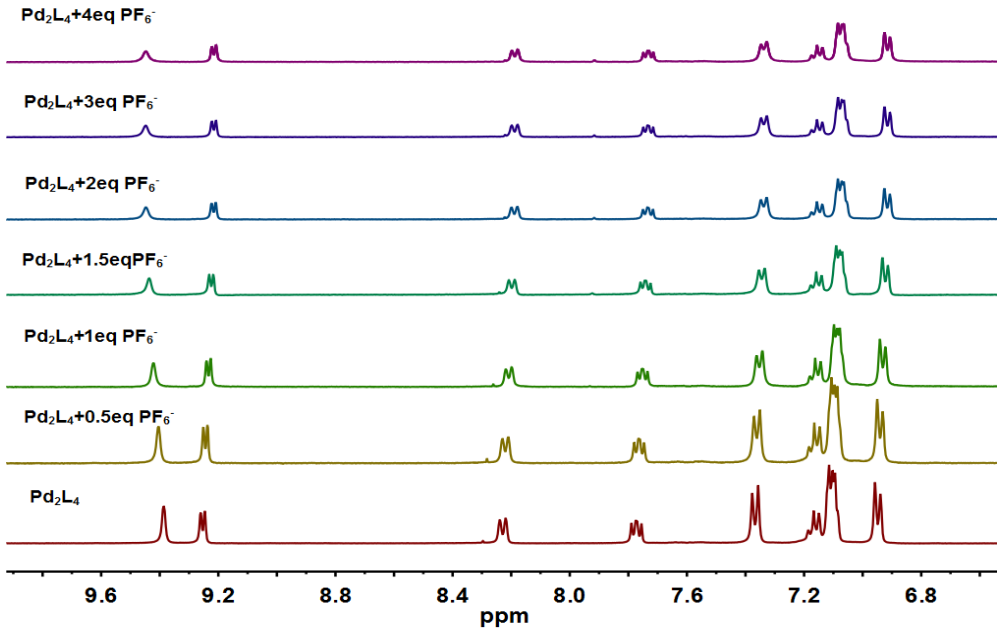

Fig. S50 ^{1}H NMR spectra of $Pd_2L_4(CF_3SO_3)_4$ with the addition of different equiv of $N(C_4H_9)_4PF_6$ (400 MHz, [D_6]DMSO, 298K)

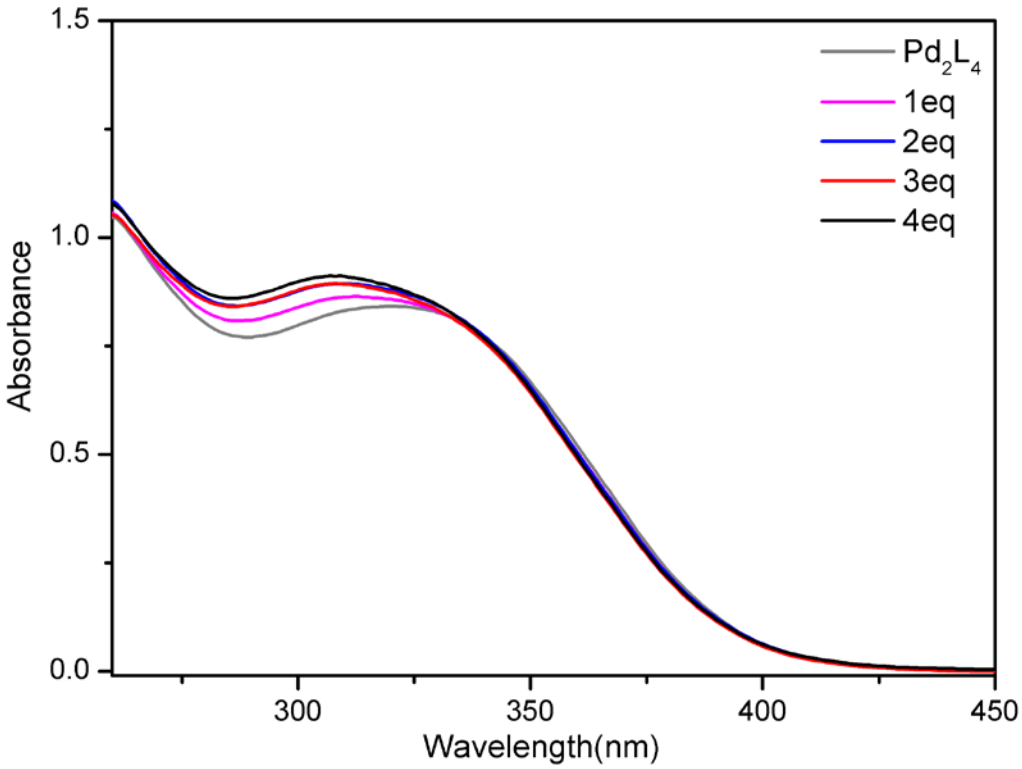

Fig. S51 UV-vis absorption spectra of $Pd_2L_4(CF_3SO_3)_4$ with the addition of different equiv of $N(C_4H_9)_4PF_6$ (c = 1.0 × 10^{-5} M)

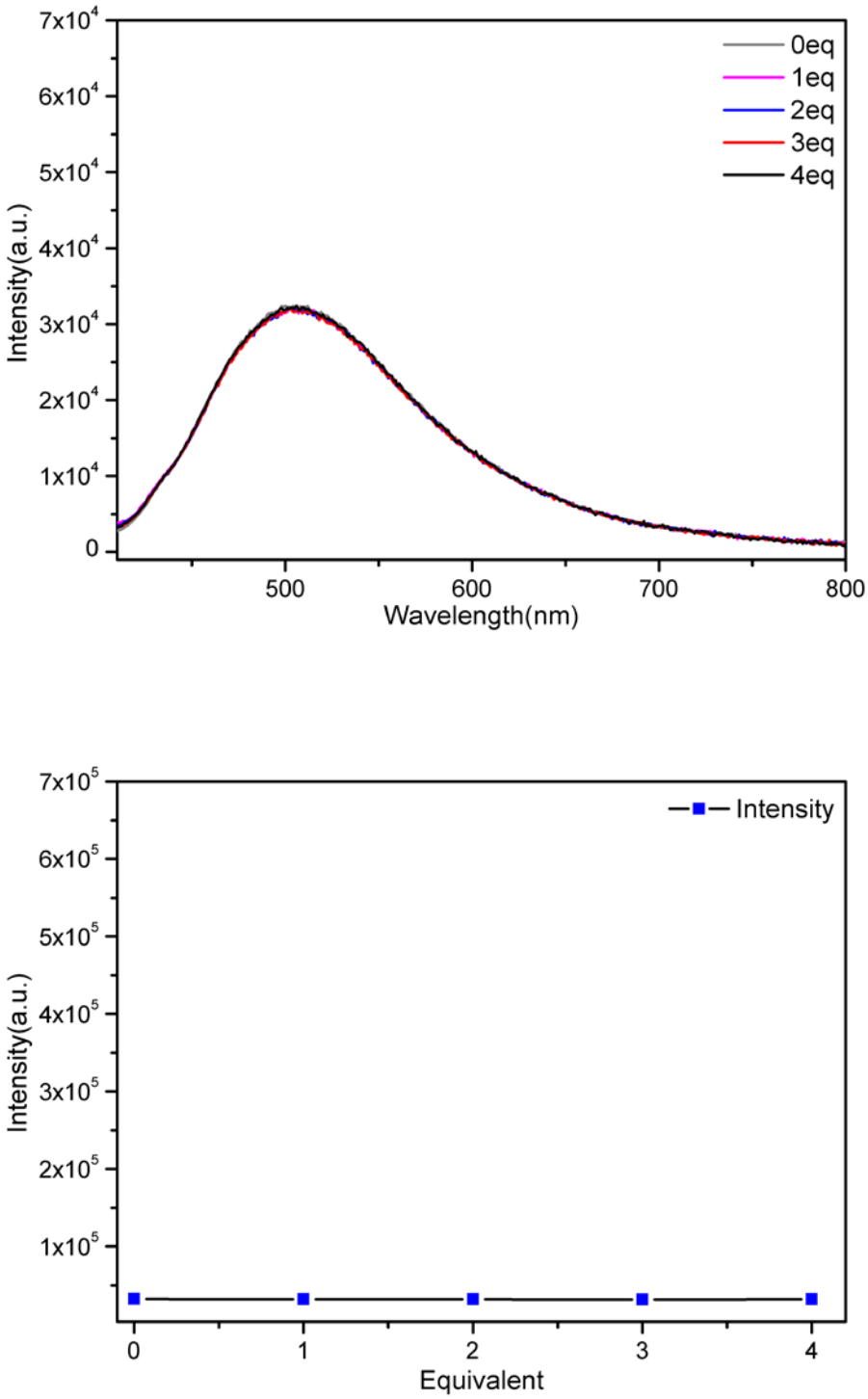

Fig. S52 Fluorescence titration spectra of $Pd_2L_4(CF_3SO_3)_4$ with the addition of different equiv of $N(C_4H_9)_4PF_6$ (1.0 × 10^{-4} M, λ_{ex} = 380 nm).

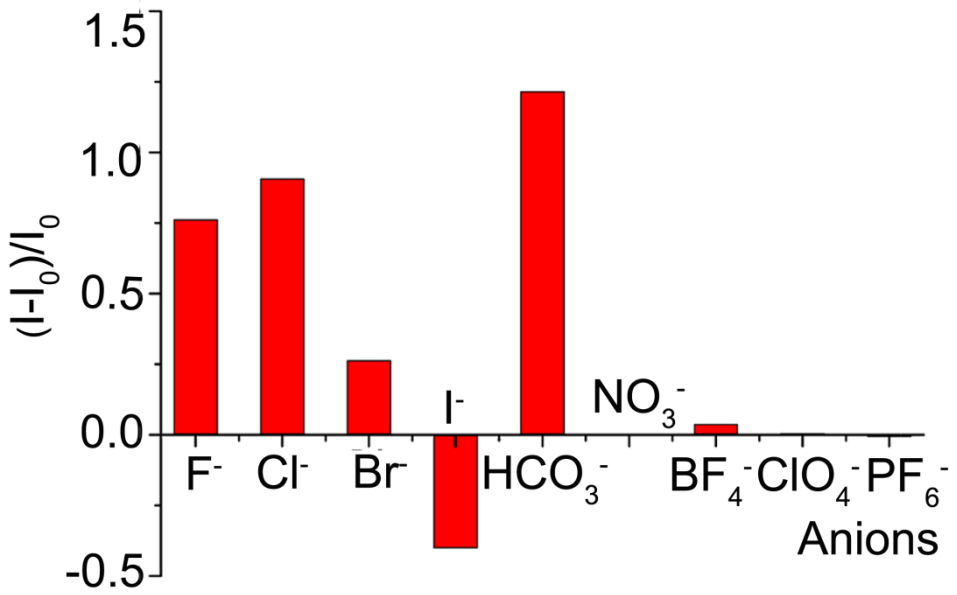

Fig. S53 The differential fluorescence intensity at λem = 504nm before (I_0) and after (I) the addition of 4 equiv of tetrabutylammonium (TBA) salts with different anions.

4. Supporting References

S1. Sheldrick G. M., *Acta Crystallogr. Sect. A*, 2008, **64**, 112-122.

S2. Spek A. L., *J. Appl. Crystallogr.*, 2003, **36**, 7-13.